Acta Pharmaceutica Sinica B 2022;12(12):4309–4326

Chinese Pharmaceutical Association
Institute of Materia Medica, Chinese Academy of Medical Sciences

Acta Pharmaceutica Sinica B

www.elsevier.com/locate/apsb
www.sciencedirect.com

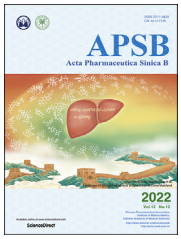

REVIEW

Harnessing the cyclization strategy for new drug discovery

Kai Tang, Shu Wang, Wenshuo Gao, Yihui Song*, Bin Yu*

School of Pharmaceutical Sciences, Zhengzhou University, Zhengzhou 450001, China

Received 10 August 2022; received in revised form 7 September 2022; accepted 23 September 2022

KEY WORDS

Ring cyclization;
Spirocyclization;
Macrocyclization;
Conformational constraint;
Lead generation;
New drug discovery

Abstract The design of new ligands with high affinity and specificity against the targets of interest has been a central focus in drug discovery. As one of the most commonly used methods in drug discovery, the cyclization represents a feasible strategy to identify new lead compounds by increasing structural novelty, scaffold diversity and complexity. Such strategy could also be potentially used for the follow-on drug discovery without patent infringement. In recent years, the cyclization strategy has witnessed great success in the discovery of new lead compounds against different targets for treating various diseases. Herein, we first briefly summarize the use of the cyclization strategy in the discovery of new small-molecule lead compounds, including the proteolysis targeting chimeras (PROTAC) molecules. Particularly, we focus on four main strategies including fused ring cyclization, chain cyclization, spirocyclization and macrocyclization and highlight the use of the cyclization strategy in lead generation. Finally, the challenges including the synthetic intractability, relatively poor pharmacokinetics (PK) profiles and the absence of the structural information for rational structure-based cyclization are also briefly discussed. We hope this review, not exhaustive, could provide a timely overview on the cyclization strategy for the discovery of new lead compounds.

*Corresponding authors.
E-mail addresses: songyihui@zzu.edu.cn (Yihui Song), yubin@zzu.edu.cn (Bin Yu).

Peer review under the responsibility of Chinese Pharmaceutical Association and Institute of Materia Medica, Chinese Academy of Medical Sciences

https://doi.org/10.1016/j.apsb.2022.09.022

1. Introduction

From the perspective of drug discovery, the optimization of the lead compounds for improving potency, selectivity, and other drug-like properties is one of the challenges facing the medicinal chemists[1]. In general, the lead compounds with five or more rotatable bonds have many molecular conformations and are difficult to bind to the targets in the correct conformation, thereby reducing the affinity of the lead compounds to the targets of interest[2]. Unrestricted conformations may also bind to other biomolecules, resulting in poor selectivity and unexpected toxicity[3,4]. Therefore, it is necessary to restrict the conformation of the lead compounds and lock it on the pharmacodynamic conformation that interacts with the target molecules, thereby improving the affinity and selectivity of the compounds[5,6].

The binding of the drug to its receptor is a complex thermodynamic process[7,8]. It is estimated that the entropy loss of a small molecule ligand with a molecular weight of 1000 at room temperature during this process is 258 kJ/mol, and the entropy value decreases by 2−3 kJ/mol for every free bond that the ligand restricts[9,10]. To make the binding free energy (ΔG) between the ligand and the receptor negative ($\Delta G < 0$), the energy consumed to reduce the conformational freedom needs to be compensated by the non-bonding interaction between the molecules. In general, conformation restriction on the ligand can reduce the compensation of entropy and increase the binding affinity of the ligand.

There are many approaches to restrict the conformation of the molecule including cyclization, introducing different rigid groups such as double bond, triple bond, amide as well as benzene ring, and increasing steric hindrance by introducing methyl or cyclopropyl[11−14]. Among these approaches, the cyclization strategy is the most direct method of conformational restriction and has been widely used in drug design, particularly for the peptide design[15−26]. In this review, we briefly summarize the cyclization strategies for new drug discovery (Fig. 1), including ring fusion, chain cyclization, spiro cyclization as well as macrocyclization, and further highlight their advantages such as improving the potency and selectivity, enhancing the pharmacodynamic and kinetic properties of small molecule compounds, and increasing the structural novelty and complexity of compounds.

2. Using the cyclization strategy for new drug discovery

As a commonly used approach, the cyclization strategy has been widely used in drug discovery. Here we summarize some recent representative examples in detail to present applications of diverse cyclization approaches in drug design, including the introduction of fused rings, macrocycles, spiro rings, etc. These conformational restriction strategies have been proved to significantly improve the drug-like properties of lead compounds.

2.1. *Fused cyclization in drug discovery*

As a heme-containing enzyme that catalyzes the oxidation of L-tryptophan (L-Trp), indoleamine 2,3-dioxygenase 1 (IDO1) has long been of interest to researchers due to its role in immunotherapy[27−29]. To date, eleven small-molecule IDO1 inhibitors have advanced into clinical trials, including NLG909 for the treatment of advanced solid tumors (Clinical Trials.gov Identifier: NCT05469490)[30]. In the discovery process of clinical candidate NLG-919 (Fig. 2, IDO1 IC_{50} = 28 nmol/L), Newlink researchers designed tricyclic imidazoisoindoles based on 4-PI (**1**, IDO1 IC_{50} = 28 μmol/L) incorporating a methylene linker at its N1 and 2′-positions, which was proved to be able to improve potency (**2**, IDO1 IC_{50} = 5.7 μmol/L)[31]. The X-ray structure of NLG-919 bound to IDO1 displays that due to the reduction of rotatable bonds, the fused imidazoisoindole core coordinates to the heme iron with higher affinity, and the phenyl group also fits in the hydrophobic pocket better.

Furazanyl hydroxyamidine **3** was known to be an effective IDO1 heme-binding inhibitor (Fig. 3, IDO1 IC_{50} = 1.5 μmol/L, HeLa cell IC_{50} = 1.0 μmol/L), Zhang et al.[32] further designed a series of benzo-fused analogs with varied ring sizes and identified the 6,5-fused oxindole as an optimal motif, and its (*S*)-isomer **4** showed excellent inhibitory effects in both enzymatic and cellular assays (IDO1 IC_{50} = 0.052 μmol/L, HeLa cell IC_{50} = 0.087 μmol/L). Cheng et al.[33] previously identified phenyl benzenesulfonyl hydrazide **5** as a potent IDO1 inhibitor *in vitro* (Fig. 3, IDO1 IC_{50} = 130 nmol/L), but further pharmacokinetic analysis indicated compound **5** was not stable enough with 37% of oral bioavailability and did not inhibit tumor growth. Therefore, further optimization for improving the pharmacokinetic profile was carried out, resulting in cyclized compound **6**, a potent and orally bioavailable IDO1 inhibitor with 73% of tumor growth delay in the implanted CT26 model (IDO1 IC_{50} = 36 nmol/L, F = 59%)[34]. Accordingly, compound **6**, an immunotherapeutic anticancer agent, deserved further preclinical evaluation.

As the first discovered histone demethylase, lysine specific demethylase 1 (LSD1) is responsible for mono- and di-methyl modification of histone H3K4 and H3K9 through flavin adenine dinucleotide (FAD)-dependent enzymatic oxidation, being a promising therapeutic target for cancer therapy[35−38]. There are two types of LSD1 inhibitors reported so far, irreversible inhibitors covalently bonding with the cofactor FAD and reversible inhibitors competing with the substrate binding. Irreversible inhibitors, such as TCP and compound **8** (Fig. 4), can react with the flavin motif of FAD to form a tight-binding adducts and inhibit other homologous FAD-dependent enzymes LSD2 and MAOs[39,40].

In 2017, Ji et al.[41] reported a series of conformationally restricted TCP-based derivatives through enantioselective synthesis and chiral resolution. The structure−activity relationships (SARs) studies demonstrated that most *cis* isomers were found to be more potent than the corresponding *trans* isomers, and both of the most potent compounds **7a** and **7b** (IC_{50} = 6.4 and 2.2 nmol/L, respectively) showed over 3000-fold increase in LSD1 inhibition compared to TCP and excellent selectivity over MAO-A/B (IC_{50} > 100 μmol/L). As shown in the co-crystal structure of compound **8** with LSD1 (PDB code: 2XAQ), there was a relatively large space between the phenyl ring of FAD-adduct and nearby residues to accommodate substituents or rings[42]. Further cyclization led to the generation of novel indoline derivatives. The representative compound **9** showed potent inhibitory activity against LSD1 (IC_{50} = 24.43 nmol/L) and excellent selectivity over MAO-A/B (>4000-fold) and LSD2 (>200-fold). Furthermore, **9** demonstrated a moderate T/C value of 30.89% *in vivo*.

Compared to irreversible LSD1 inhibitors, reversible LSD1 inhibitors SP-2577 and CC-90011 have already entered clinical trials[43]. Zhao et al.[44,45] restricted the conformation of compound **10** (SP-2509, the analog of SP-2577) by replacing the acetophenone moiety with 2,3-dihydro-1*H*-inden-1-one moiety. In consequence, the corresponding products **11a** and **11b** showed nearly 10-fold increased inhibitory activity (IC_{50} = 1.4 and 1.7 nmol/L, respectively). Based on the binding mode of compound **12** with

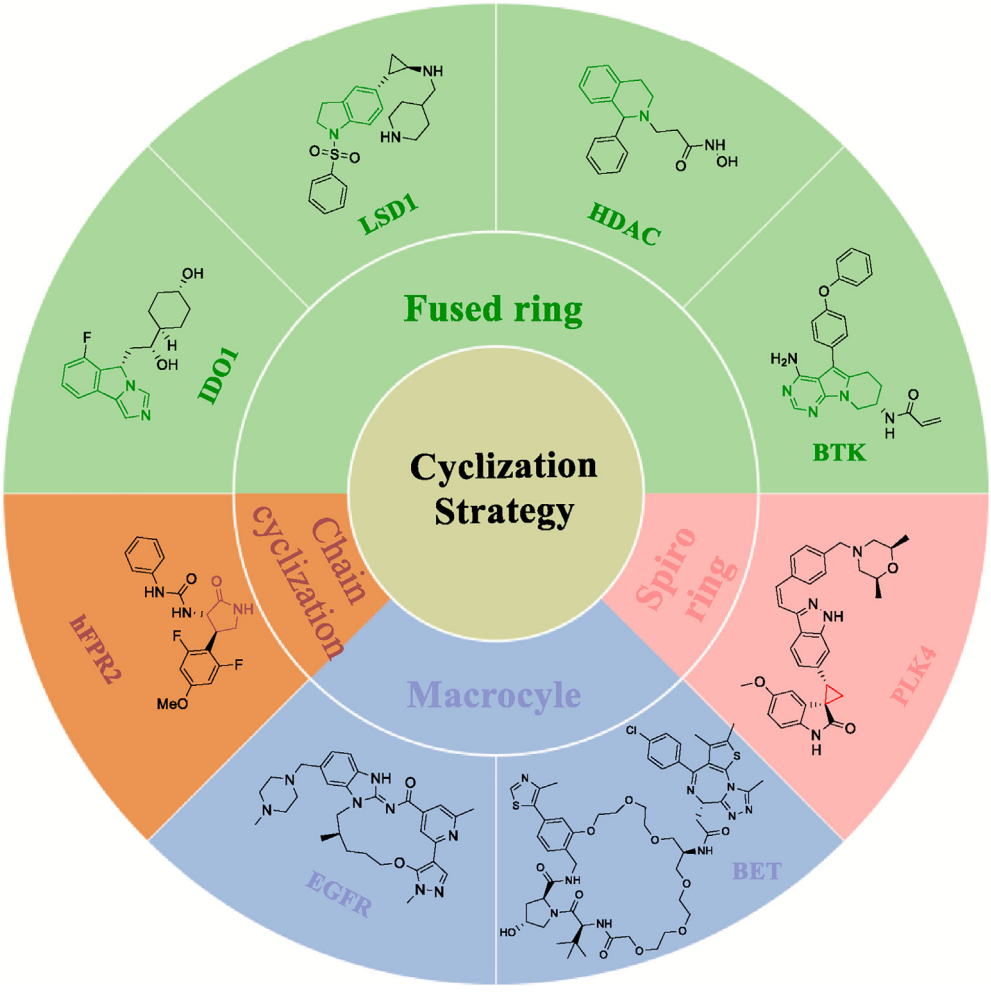

Figure 1 Selected conformationally constraint lead compounds designed based on the cyclization strategy.

LSD1, Cheng et al.[46] employed the cyclization strategy to design novel tetrahydroquinoline-based LSD1 inhibitors (Fig. 5), which not only maintained the U-shaped conformation but also reserved the hydrogen bond interaction between terminal alkaline fragment with D555 and the $\pi-\pi$ stacking between arylthiophene fragment and FAD. Compound **13** exhibited excellent LSD1 inhibition (IC_{50} = 55 nmol/L), good selectivity over MAO-A/B and moderate antiproliferative activity against MGC-803 cells (IC_{50} = 1.13 μmol/L). They also designed a series of benzofuran derivatives based on the cyclization strategy of compound **14** (IC_{50} = 134 nmol/L). Similarly, the original hydrogen bond interactions between the piperazine ring with D555 and $\pi-\pi$ stacking between the 4-cyanophenyl group and FAD were still maintained. In particular, compound **15** showed excellent LSD1 inhibition with an IC_{50} value of 65 nmol/L and an antiproliferative effect against cancer cell lines overexpressing LSD1[47].

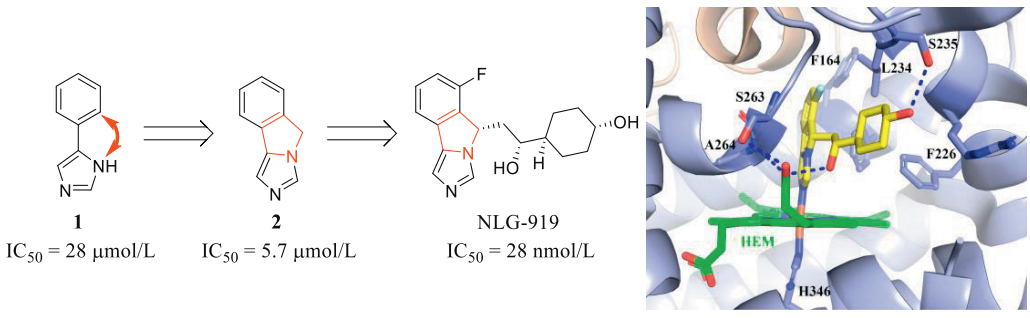

Figure 2 The optimization of NLG-919 using the cyclization strategy (PDB code: 6O3I). The inhibitor NLG-919 is displayed in the yellow stick. The H-bonding interactions between NLG-919 and the IDO1 protein matrix are indicated by the blue dotted lines.

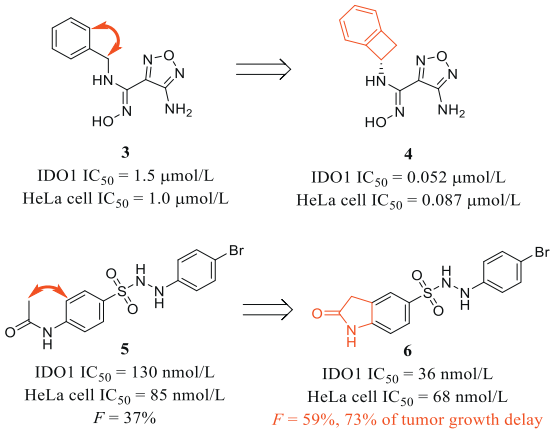

Figure 3 The representative cyclization examples of IDO1 inhibitors.

As critical epigenetic modulators of gene expression, histone deacetylases (HDACs) catalyze the removal of acetyl moieties from lysine in histones and non-histone substrates and have been validated as an important class of epigenetic drug targets for the treatment of many cancers, inflammatory and neurodegenerative diseases[48–50]. So far, there are four FDA-approved HDAC inhibitors (HDACis) for the treatment of multiple myeloma and peripheral or cutaneous T-cell lymphoma[51].

Taha et al.[52] developed a novel series of tetrahydroisoquinoline HDAC8 inhibitors based on previous tertiary amine **16** (Fig. 6A). The SAR studies suggested that compound **17** connecting the tertiary amine and the phenyl moiety displayed the highest HDAC inhibition and 135-fold selectivity over HDAC1, which would be further optimized by varying the substitution at the C1 position of the tetrahydroisoquinoline scaffold.

McClure et al.[53] disclosed the allosteric hydrazide-containing HDACs inhibitor **18** in 2016 (Fig. 6B). Although the superior inhibitory activity of compound **18**, its α,β-unsaturated ketone as a "Michael receptor" might induce promiscuous cellular responses due to the reaction with thiol groups. So they continued to modify the cinnamamide group with an indole ring to deactivate the Michael acceptor[54]. Finally, the cyclic compound **19** exhibited improved potency by a factor of 2–5 than **18** against HDAC enzymes (IC_{50} = 0.43–18.54 nmol/L), excellent PK profile (F = 112%) and outstanding *in vivo* anti-AML activity (TGI = 78.9%).

Bruton's tyrosine kinase (BTK), a nonreceptor tyrosine kinase belonging to the Tec family of cytoplasmic tyrosine kinases, plays an important role in the pathogenesis of B-cell lymphomas, and increasing evidence suggests that BTK is a validated therapeutic target for the treatment of hematological malignancies[55–58].

In 2019, Guo et al.[59] synthesized a novel series of compounds with a pseudo pyrimidinone ring through an intramolecular hydrogen bond, and these compounds displayed good BTK potency (Fig. 7A). Encouragingly, the ring-merged compound BGB-3111 (**20**) possessed unexpected BTK potency (IC_{50} = 0.3 nmol/L), high selectivity over other kinases as well as outstanding *in vivo* efficacy in OCI-LY10 xenograft models. BGB-3111 (Zanubrutinib) is currently being evaluated in clinical trials.

Ibrutinib (**21**), the first-generation BTK inhibitor, was approved by FDA in 2013 for the treatment of mantle cell lymphoma (MCL) and chronic lymphocytic leukemia (CLL)[60]. As shown in Fig. 7B, ibrutinib is an irreversible inhibitor *via* a covalent bond formed by its acrylamido moiety with C481 of BTK protein (PDB code: 5P9J)[61]. To obtain novel BTK inhibitors, Zhao et al.[62] merged the piperidine ring and the pyrazolo[3,4-*d*]pyrimidine moiety of **21** into the tricyclic backbone. The critical covalent interaction and three H-bonding interactions with Y474, E475, and M477, were not affected. Finally, they obtained a new BTK inhibitor **22** with comparable potency as ibrutinib (BTK IC_{50} = 0.4 nmol/L, TMD8 cell IC_{50} = 16 nmol/L) and effective tumor growth suppression in the TMD8 xenograft model.

Based on previously reported triazine analog **23** (Fig. 7C), Kawahata et al.[63] cyclized the N atom at 1-position and the NH at 2-position of the triazine ring without causing the loss of

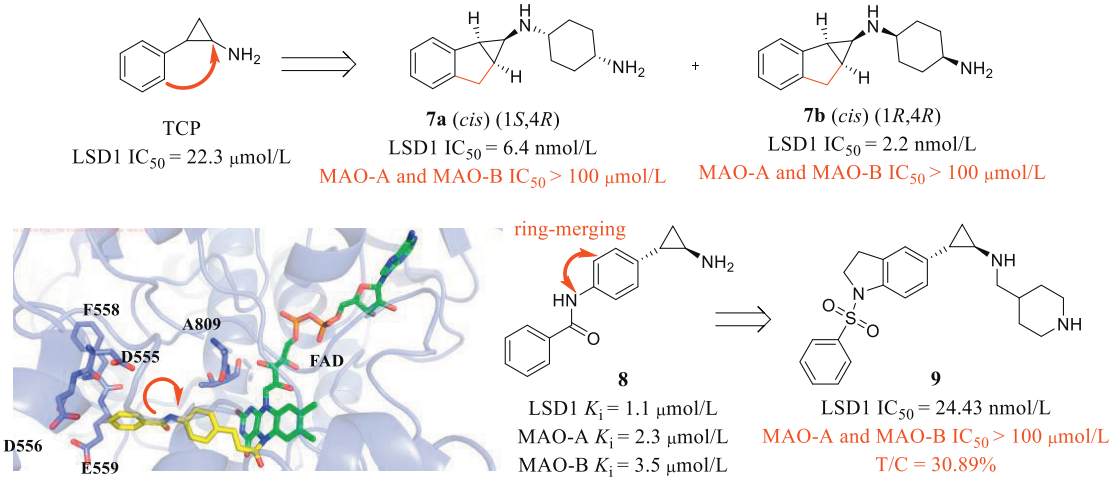

Figure 4 Rational design of novel irreversible LSD1 inhibitors. Compound **8** is displayed in the yellow stick. The FAD is displayed in the green stick (PDB code: 2XAQ).

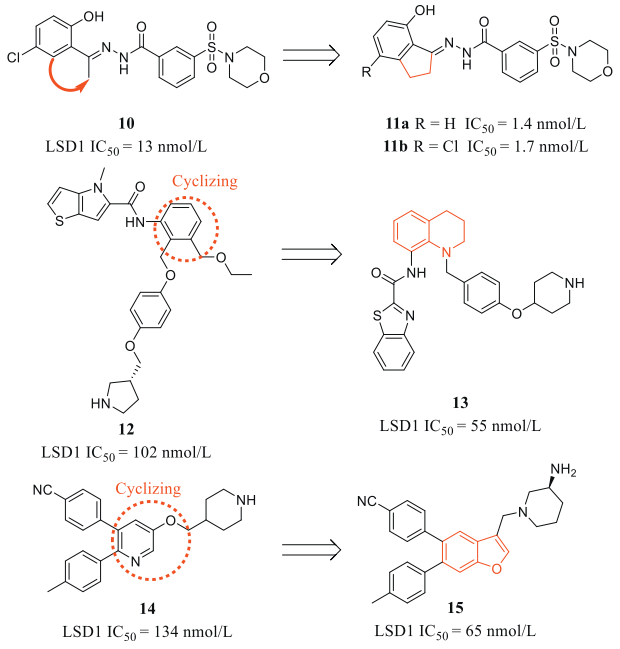

10
LSD1 IC_{50} = 13 nmol/L

11a R = H IC_{50} = 1.4 nmol/L
11b R = Cl IC_{50} = 1.7 nmol/L

12
LSD1 IC_{50} = 102 nmol/L

13
LSD1 IC_{50} = 55 nmol/L

14
LSD1 IC_{50} = 134 nmol/L

15
LSD1 IC_{50} = 65 nmol/L

Figure 5 Design of reversible LSD1 inhibitors based on the cyclization strategy.

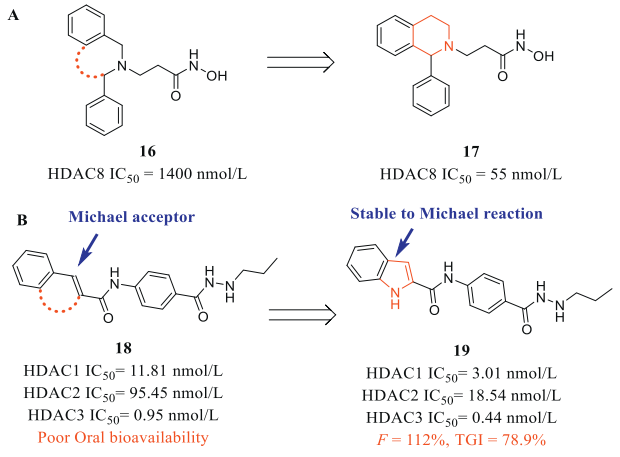

16
HDAC8 IC_{50} = 1400 nmol/L

17
HDAC8 IC_{50} = 55 nmol/L

18
HDAC1 IC_{50}= 11.81 nmol/L
HDAC2 IC_{50}= 95.45 nmol/L
HDAC3 IC_{50}= 0.95 nmol/L
Poor Oral bioavailability

19
HDAC1 IC_{50}= 3.01 nmol/L
HDAC2 IC_{50}= 18.54 nmol/L
HDAC3 IC_{50}= 0.44 nmol/L
F = 112%, TGI = 78.9%

Figure 6 The representative cyclization examples of HDACs inhibitors.

inhibitory activity, which led to the discovery of AS-1763 (**24**), a potent, selective, and orally available noncovalent BTK inhibitor (IC_{50} = 0.4 nmol/L). Currently, AS-1763 has advanced into phase 1 clinical trial for treating chronic lymphocytic leukaemia (ClinicalTrials.gov Identifier: NCT05365100).

The CXC chemokine receptor 2 (CXCR2) is essential in the recruitment of myeloid-derived suppressor cells (MDSCs) to the tumor microenvironment, making it an attractive drug target for cancer immunotherapy[64]. SB-332235 (**25**, Fig. 8) featuring a sulfonamide/sulfone moiety adjacent to phenol serves as a starting point for further modification[65]. Dong et al.[66] designed a series of unsaturated benzocyclic sulfone derivatives based on the cyclization strategy. Extensive SAR studies resulted in the discovery of a novel potent CXCR2 antagonist **26** with an IC_{50} value of 34 nmol/L. Molecular docking analysis showed that both the non-

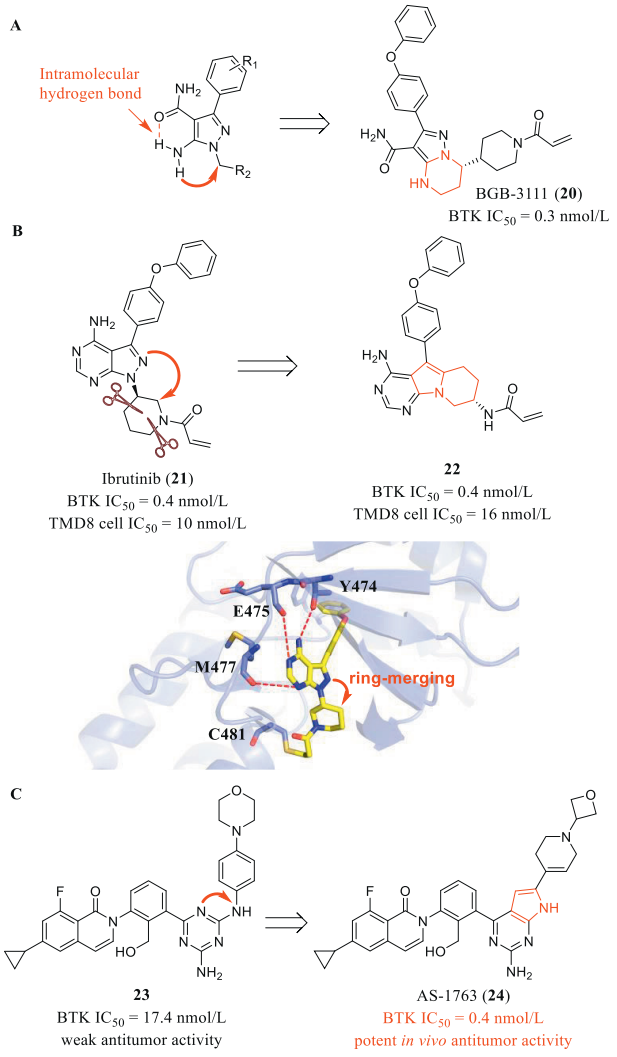

Ibrutinib (**21**)
BTK IC_{50} = 0.4 nmol/L
TMD8 cell IC_{50} = 10 nmol/L

22
BTK IC_{50} = 0.4 nmol/L
TMD8 cell IC_{50} = 16 nmol/L

BGB-3111 (**20**)
BTK IC_{50} = 0.3 nmol/L

23
BTK IC_{50} = 17.4 nmol/L
weak antitumor activity

AS-1763 (**24**)
BTK IC_{50} = 0.4 nmol/L
potent *in vivo* antitumor activity

Figure 7 The representative cyclization examples of BTK inhibitors. The inhibitor **21** is displayed in the yellow stick (PDB code: 5P9J). The H-bonding interactions between **21** and the BTK protein are indicated by the red dotted lines.

cyclic SB-332235 and cyclic **26** occupied the allosteric site of CXCR2 and formed H-bonding interactions with S81, T83, D84 and K320, respectively. In particular, compound **26** did not induce the steric effect compared to SB-332235.

P2Y12 receptor, an important antithrombotic target, plays a crucial role in the amplification of platelet activation, aggregation and stable thrombosis[67,68]. Among the reported antagonists, the clinical studies of AZD1283 (Fig. 9) were terminated due to the poor metabolic stability of the ester[69]. Yang et al. designed a series of novel bicyclic pyridine analogs of AZD1283 *via* cyclization of the ester group to the *ortho*-methyl, which generally possessed comparable enzymatic inhibitory activity and improved metabolic stability[70]. Importantly, compound **27** exhibited significantly enhanced metabolic stability than AZD1283 in rat and human microsomes.

TRAF-2 and NCK-interacting kinase (TNIK) is one of the most promising targets involved in the Wnt/β-catenin pathway[71–73]. Recently, Li et al.[74] obtained a hit compound **28** (Fig. 10, IC_{50} = 1.337 μmol/L) by virtual screening, further conformation restriction by cyclizing its carbamoyl group and

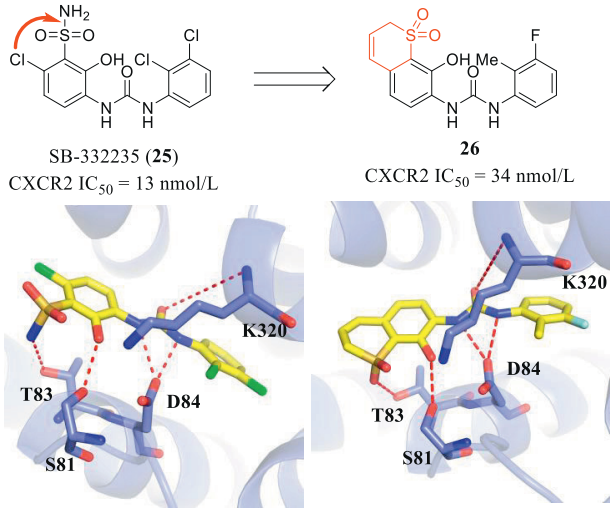

Figure 8 Rational design of benzocyclic sulfone derivatives as CXCR2 antagonists. The inhibitors **25** and **26** are displayed in the yellow stick. The H-bonding interactions between inhibitors and the CXCR2 protein are indicated by the red dotted lines (PDB code: 6LFL).

methoxy group and lengthening the phenylamine group led to the discovery of the most active compound **29** (IC_{50} = 0.026 μmol/L) with high selectivity and good PK properties. Moreover, **29** showed excellent antitumor efficacy in the HCT116 xenograft mouse model.

Focal adhesion kinase (FAK) is a tyrosine kinase overexpressed in highly aggressive and metastatic cancers including acute myeloid leukemia (AML)[75]. While oncogenic mutations in FMS-like tyrosine kinase 3 (FLT3) occur most frequently in AML[76]. A recent study indicated that the FAK inhibitors targeting FLT3 could be used to overcome resistance driven by FLT3 mutations[77,78]. Therefore, Cho et al.[79] utilized the fused thieno[3,2-*d*]pyrimidine ring as a novel scaffold for developing FAK inhibitors based on the reported PF-562271 (Fig. 11A), of which the hydrophobic thiophene moiety could mimic the trifluoromethyl group. After several rounds of structural optimizations, they finally obtained a promising dual inhibitor **30**, which displayed excellent inhibitory activities against FLT3-D835Y mutant (IC_{50} < 0.5 nmol/L) and FAK (IC_{50} = 9.7 nmol/L). The molecular docking model with FAK protein (PDB code: 2JKK) revealed that compound **30** formed two hydrogen bonds with C502, and its thiophene moiety also contributed to enhanced hydrophobic interactions (Fig. 11B). The docking results with FLT3 protein (PDB code: 5X02) showed that **30** also formed the H-bonding interaction with C694 in the hinge region (Fig. 11C).

Enhancer of zeste homolog 2 (EZH2) is a histone methyltransferase, which regulates the normal physiological function of cells by catalyzing the methylation of lysine 27 of histone H3 (H3K27) to control the expression of various genes[80–82]. Based on the EZH2 inhibitor **31** (Fig. 12, IC_{50} = 5700 nmol/L), Kung et al.[83] found that the cyclization of the amide linker can improve the binding property of **31**. Subsequent structural optimizations resulted in the lactam analog **32**, which showed significantly improved ligand efficiency (K_i = 0.7 nmol/L) and potency (IC_{50} < 5 nmol/L) and robust *in vivo* antitumor effects.

The receptor activator of nuclear factor Kappa-B ligand (RANKL) is a member of the tumor necrosis factor superfamily, a key factor responsible for osteoclast differentiation, activation and apoptosis. The small-molecule inhibitors of RANKL can be used in the treatment of osteoporosis[84–86]. In 2019, Jiang et al.[87] reported that the compound Y1599, a potent small-molecule RANKL inhibitor, showed good osteoclastogenesis inhibition *in vitro* (Fig. 13, 32% at 1 μmol/L) but failed to exhibit oral efficacy *in vivo*. Interestingly, cyclization of compound Y1599 gave the *β*-carboline analog Y1693, which exhibited excellent osteoclastogenesis inhibition (89% at 1 μmol/L) and low toxicity. Y1693 markedly reversed OVX-induced osteoporosis after oral administration and could be used as a promising candidate for antiresorptive therapies[88].

2.2. *Chain cyclization in drug discovery*

Chain cyclization is another widely used strategy in drug design. As shown in Fig. 14, based on the antipsychotic drug chlorpromazine, many derivatives have been developed. Considering the flexibility of the side chain, cyclizing the terminal dimethylamino group in chlorpromazine may reduce the flexibility and give methdilazine and prochlorperazine with improved antiemetic effect[89,90].

Based on the structure of chidamide (**33**) approved by the NMPA for treating recurrent and refractory peripheral T-cell lymphoma in 2015[91], Cui et al.[92] optimized its amide region of **33** by forming a six-member ring to improve its PK profiles and *in vivo* efficacy (Fig. 15). Among these compounds, the most potent compound **34** (HDAC1 IC_{50} = 84.9 nmol/L) exhibited significantly improved oral bioavailability (F = 92%) and significant *in vivo* antitumor efficacy in a TMD-8 xenograft model (TGI = 77%) without obvious toxicity. The docking results showed that the cyclization did not impact original key interactions between chidamide with HDAC1, including the H-

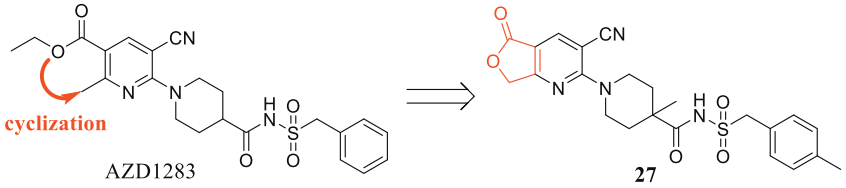

Figure 9 The discovery of lactone analog **27** of AZD1283 *via* the cyclization strategy.

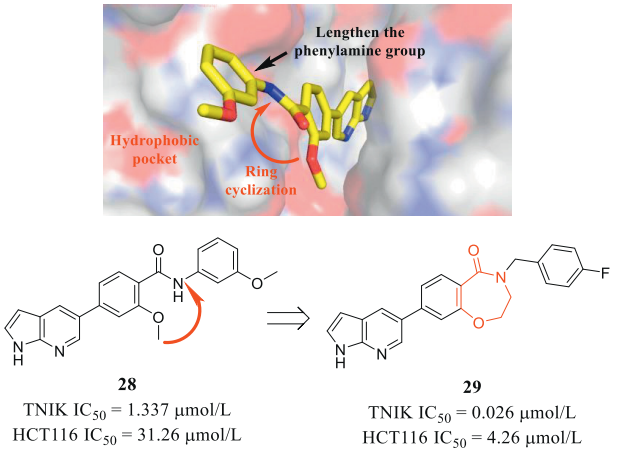

Figure 10 The discovery of novel selective TNIK inhibitors *via* cyclization strategy (PDB code: 5AX9). The inhibitor **28** is displayed in the yellow stick.

bonding with D168 and $\pi-\pi$ stacking interactions with F141 as well as F198.

FPR2 can resolve chronic inflammation and promote the wound healing processes due to its important role in both host defense and inflammation[93–95]. In 2019, Asahina et al.[96] firstly obtained the carbamoyl derivative **35** with excellent potency (Fig. 16, IC_{50} = 4 nmol/L). The subsequent introduction of a conformation-restricted pyrrolidinone moiety led to a series of lactam derivatives, and the final optimization of lactam substituents generated the compound **36** (BMS-986235, IC_{50} = 0.4 nmol/L), an FPR2 selective agonist with 7000-fold selectivity over FPR1. While treated with **36** in a mouse heart failure model, the corresponding cardiac structure and functional improvements were observed.

Akt (protein kinase B, PKB), a serine/threonine kinase that belongs to the AGC family of kinases, is an important component in the PI3K/Akt signaling pathway[97–99]. GSK-795 is an ATP-competitive Akt inhibitor with excellent PK profiles and now is in early clinical trials[100]. Dong et al.[101] designed a series of 3,4-disubstituted piperidine derivatives based on GSK-795 by cyclizing its amino group with the methylene moiety of the benzyl group, which generally showed excellent *in vitro* and *in vivo* antitumor efficacy but with high toxicity (Fig. 17). Further optimization by introducing diverse side chains ultimately led to the identification of compound **37**. The compound not only showed increased inhibitory activity against Akt1 (IC_{50} = 1.4 nmol/L) and *in vivo* antitumor efficacy (TGI >90%), but also possessed remarkably improved safety profiles (MTD >80 mg/kg).

2.3. *Spirocyclization in drug discovery*

Due to the three-dimensional structural characteristic and conformational restriction, spiro compounds can bind to the

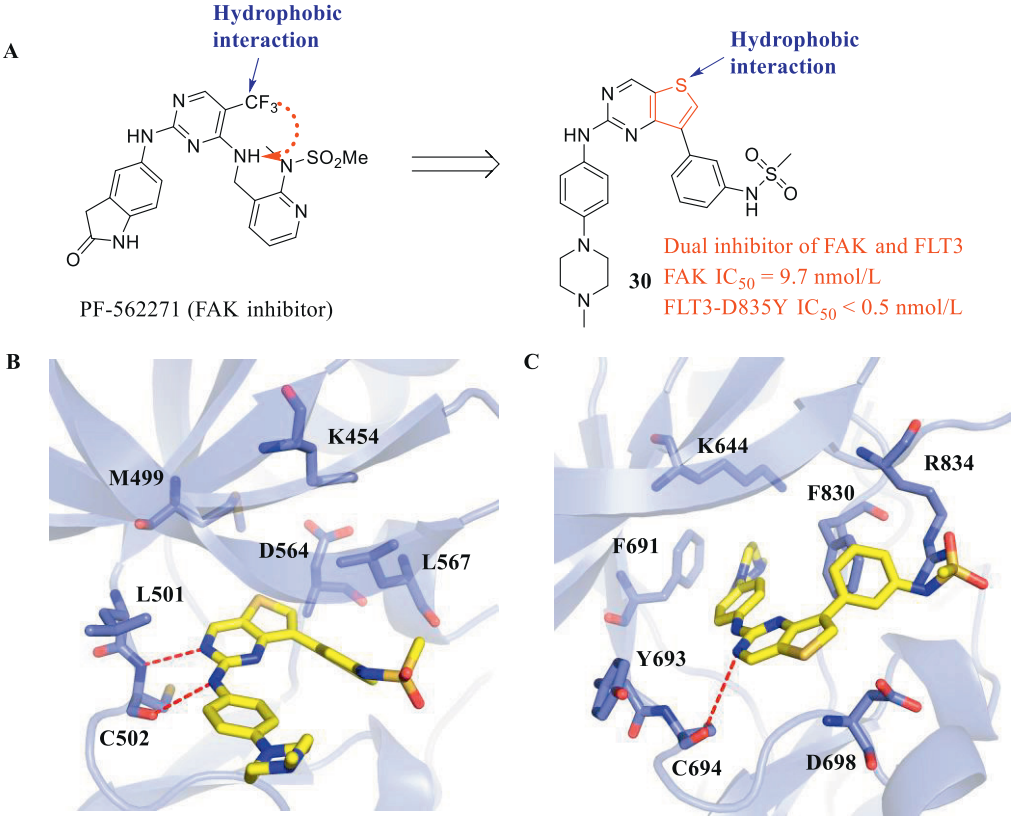

Figure 11 (A) The discovery of thieno[3,2-*d*]pyrimidine **30** as the dual inhibitor of FAK and FLT-3. (B) Proposed docking model of **30** with FAK. The inhibitor **30** is displayed in the yellow stick. The H-bonding interactions between **30** and the FAK protein are indicated by the red dotted lines. (C) Proposed docking model of **30** with FLT3. The H-bonding interactions between **30** and the FLT3 protein matrix are indicated by the red dotted lines.

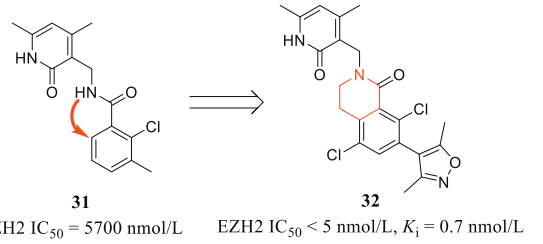

Figure 12 The discovery of novel EZH2 inhibitor **32** *via* the cyclization strategy.

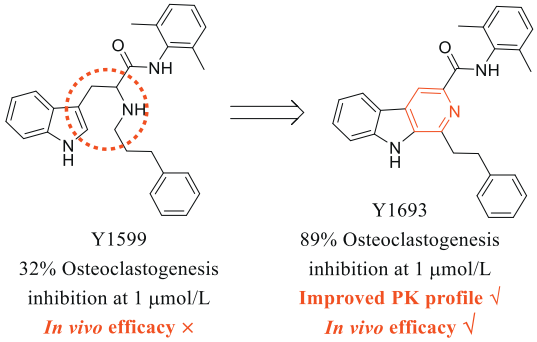

Figure 13 The discovery of novel orally active RANK inhibitor Y1693 *via* the cyclization strategy.

target protein in a lower entropy[102]. The introduction of conformational restriction by spiro ring formation, can not only modulate binding potency and specificity but also potentially improve bioavailability and metabolic stability. Furthermore, the conformational restriction by spirocyclization may reduce off-target activities[103,104]. The fraction of sp^3 carbons and chiral carbon count have been used as descriptors of molecular complexity, thus spirocyclization can provide a useful method of increasing molecular complexity and may offer greater benefits than the introduction of flat rings[105].

Polo-like kinase 4 (PLK4) is present in proliferating tissues and up-regulated in breast cancer, high PLK4 levels are associated with poor outcomes[12,106–108]. Pauls et al.[11,109] reported the first PLK4 clinical candidate CFI-400945 *via* the bioisosteric replacement of the alkene linker of compound **38** (Fig. 18, IC_{50} = 0.61 nmol/L) with a cyclopropane ring. Compared to the indolinone **38**, this structural modification resulted in a substantial improvement in PK properties (F = 66% in dogs) without significant loss of inhibitory activity (IC_{50} = 2.8 nmol/L). Currently, the fumarate of CFI-400945 is being studied in phase II clinical trials for the treatment of advanced cancer, including breast cancer (ClinicalTrials.gov identifier: NCT04176848 and NCT03624543), prostate cancer (ClinicalTrials.gov identifier: NCT03385655) as well as acute myeloid leukemia (ClinicalTrials.gov identifier: NCT03187288, NCT01954316, NCT04730258).

Cholesteryl ester transfer protein (CETP), a glycoprotein produced primarily by the liver, could mediate the exchange of triglycerides from the very low density lipoprotein (VLDL) with cholesteryl ester from high density lipoprotein (HDL). Inhibition of CETP is considered to be one of the most effective ways for increasing high density lipoprotein-cholesterol (HDL-C) levels[110–112]. Previous studies have revealed that the binding pocket of CETP is hydrophilic, which means that the potent CETP inhibitors should be hydrophilic as well. The compounds with high lipophilic properties often impact on solubility, disposition and promiscuity, thus possessing poor drug-like properties[113–115].

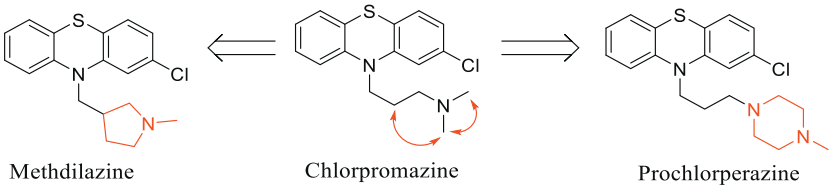

Figure 14 Drug discovery based on the chain cyclization.

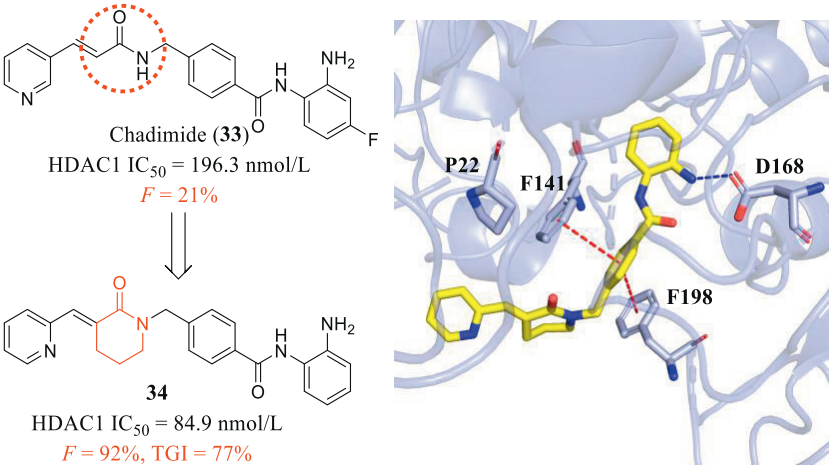

Figure 15 Representative HDACs inhibitors designed based on the ring cyclization. The inhibitor **34** is displayed in the yellow stick (PDB code: 1C3R). The $\pi-\pi$ stacking interactions between **34** and the HDAC1 protein are indicated by the red dotted lines.

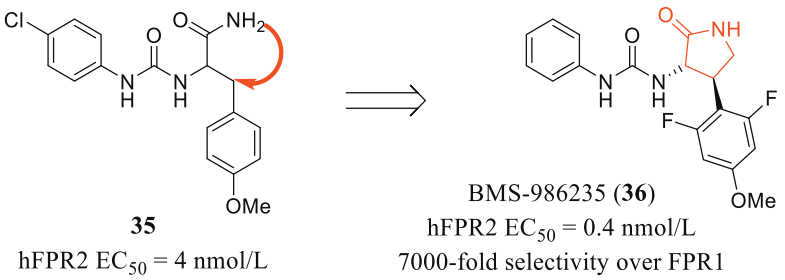

Figure 16 The discovery of the potent FPR2 selective agonist BMS-986235.

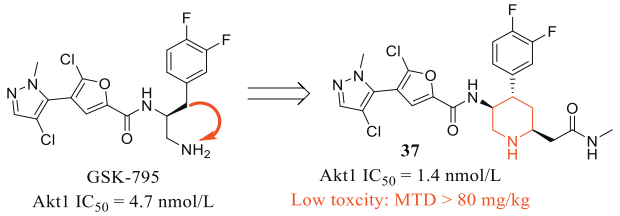

Figure 17 The discovery of 3,4,6-trisubstituted piperidine **37**.

Starting from the CETP inhibitor **39**[116], Trieselmann et al.[117] designed the analog **40** by spirocyclization of the fluorobenzyl group, this structural modification not only reduced the lipophilicity of **40** (Fig. 19, *c*log*P* = 4.6) but also increased its inhibitory activity against CETP (IC_{50} = 18 nmol/L). In addition, **40** effectively increased the level of HDL-C, decreased the level of low density lipoprotein cholesterol (LDL-C) in CETP transgenic mice and had no significant effect on blood pressure and electrocardiogram.

As a non-receptor protein tyrosine phosphatase encoded by the PTPN11 gene, the Src homology-2 domain-containing protein tyrosine phosphatase-2 (SHP2) is ubiquitously expressed and mediates several intracellular oncogenic signaling pathways[118–120]. In recent years, the development of SHP2 targeting small molecule inhibitors has been highly pursued[121–123]. The spirocyclization strategy has also been successfully employed by Novartis's researchers to develop new SHP2 allosteric inhibitors. Compound **41** showed good inhibitory activity (Fig. 20, SHP2 IC_{50} = 0.034 μmol/L), but had relatively low cellular (p-ERK IC_{50} = 0.355 μmol/L) and antiproliferative activities (KYSE520 IC_{50} = 13.49 μmol/L). After introducing the spirocyclic system carrying the exocyclic amine, the corresponding product **42** showed improved cellular efficacy (p-ERK IC_{50} = 0.012 μmol/L, KYSE520 IC_{50} = 0.167 μmol/L) due to increased lipophilicity while maintaining enzymatic activity (SHP2 IC_{50} = 0.028 μmol/L)[124].

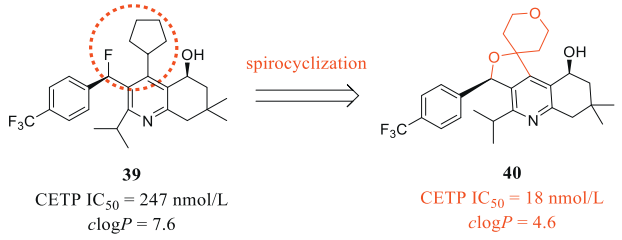

Figure 19 The discovery of the CETP inhibitor **40** *via* spirocyclization.

Plasmodium falciparum histone deacetylases (*Pf*HDACs) are widely expressed and transcribed in multiple life cycle stages of *P. falciparum* and are involved in many biological functions critical for the survival and reproduction of helminths[125,126]. Based on quisinostat, an HDAC inhibitor in phase II clinical trial[127], Li et al.[128] designed a series of novel spirocyclic hydroxamic acid derivatives by introducing the spirocyclic linker. Among them, compound **43** displayed better potency against two multi-resistant malarial parasites than quisinostat (Fig. 21, *Pf*3D7 IC_{50} = 5.2 nmol/L, *Pf*Dd2 IC_{50} = 7.1 nmol/L) and attenuated cytotoxicity against two human cell lines (HepG2 IC_{50} = 264 nmol/L, 293T IC_{50} = 241 nmol/L). Further optimization gave compound JX35, which showed a stronger triple-stage (the blood stage, liver stage, and gametocyte stage) antimalarial effect (*Pf*3D7 IC_{50} = 1.26 nmol/L, *Pf*Dd2 IC_{50} = 1.61 nmol/L), increased safety (HepG2 IC_{50} = 1.02 μmol/L, 293T IC_{50} = 1.21 μmol/L), and good pharmacokinetic properties[129].

Human mitochondrial peptide deformylase (HsPDF) is a metalloenzyme responsible for removing the N-terminal formyl group in mitochondrial proteins and plays an important role in maintaining mitochondria function[130–132]. As a naturally occurring antibiotic obtained from *Streptomyces* species, Actinonin was first reported in 2000 as an HsPDF inhibitor with a metal ion-

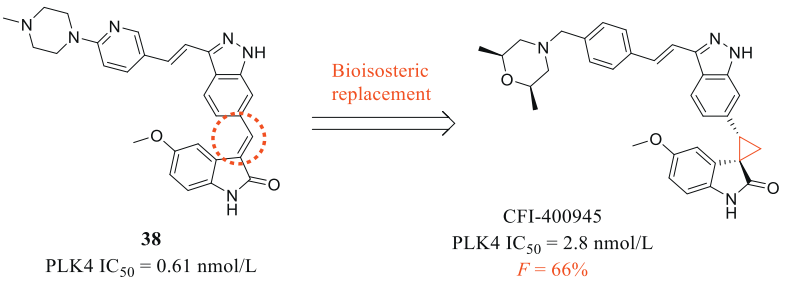

Figure 18 The discovery of the PLK4 inhibitor CFI-400945 *via* bioisosteric replacement.

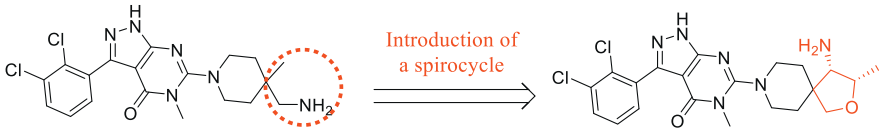

41
SHP2 IC_{50} = 0.034 μmol/L
p-ERK IC_{50} = 0.355 μmol/L
KYSE520 IC_{50} = 13.49 μmol/L

42
SHP2 IC_{50} = 0.028 μmol/L
p-ERK IC_{50} = 0.012 μmol/L
KYSE520 IC_{50} = 0.167 μmol/L

Figure 20 The discovery of the SHP2 allosteric inhibitor **42** *via* the spirocyclization.

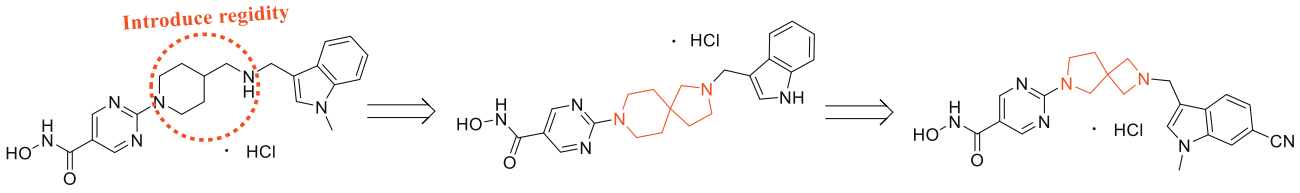

Quisinostat
*Pf*3D7 IC_{50} = 5.2 nmol/L
*Pf*Dd2 IC_{50} = 7.1 nmol/L
HepG2 IC_{50} = 42 nmol/L
293T IC_{50} = 48 nmol/L

43
*Pf*3D7 IC_{50} = 3.2 nmol/L
*Pf*Dd2 IC_{50} = 1.9 nmol/L
HepG2 IC_{50} = 264 nmol/L
293T IC_{50} = 241 nmol/L

JX35
*Pf*3D7 IC_{50} = 1.26 nmol/L
*Pf*Dd2 IC_{50} = 1.61 nmol/L
HepG2 IC_{50} = 1.02 μmol/L
293T IC_{50} = 1.21 μmol/L

Figure 21 Discovery of the *Pf*HDAC1 inhibitor JX35.

bound hydroxamic acid moiety (Fig. 22)[133]. It showed acceptable inhibitory activity (HsPDF IC_{50} = 31.6 nmol/L, HCT116 IC_{50} = 22.6 μmol/L) and provided a framework for the development of novel HsPDF inhibitors. In 2020, Hu et al.[134] reported the cyclized derivative **44** with significantly improved enzymatic activity (IC_{50} = 4.1 nmol/L) and good antiproliferative activity (HCT116 IC_{50} = 1.9 μmol/L). It also displayed better antitumor efficacy in HCT116 xenograft mouse models with tolerable toxicity compared to actinonin.

2.4. *Macrocyclization in drug discovery*

Macrocycles refer to the compounds with more than 12-membered rings, and macrocyclic compounds are believed to achieve good conformation restriction while maintaining relative molecular weight and good lipophilic efficiency (LipE)[135,136].

Crizotinib, developed by Pfizer in 2011, is an anaplastic lymphoma kinase (ALK) inhibitor[137]. However, drug resistance and difficulty in penetrating the blood−brain barrier have emerged. To overcome these defects, Pfizer developed a new generation of ALK inhibitor lorlatinib (Fig. 23, **45**) with a macrocyclic ring for

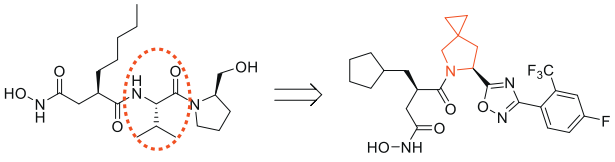

Actinonin
HsPDF IC_{50} = 31.6 nmol/L
HCT116 IC_{50} = 22.6 μmol/L

44
HsPDF IC_{50} = 4.1 nmol/L
HCT116 IC_{50} = 1.9 μmol/L

Figure 22 Discovery of the HsPDF inhibitor **44**.

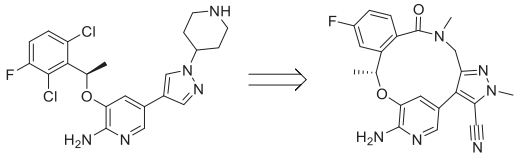

Crizotinib
ALK IC_{50} = 80 nmol/L
ALK-L1196M IC_{50} = 843 nmol/L
MDR BA/AB = 45

Lorlatinib (**45**)
ALK IC_{50} = 1.3 nmol/L
ALK-L1196M IC_{50} = 21 nmol/L
MDR BA/AB = 1.5

Figure 23 The discovery of the macrocyclic ALK inhibitor lorlatinib.

the treatment of ALK-positive lung cancer patients[138]. Compared to crizotinib (ALK IC_{50} = 80 nmol/L, ALK-1196M IC_{50} = 843 nmol/L), the macrocyclic inhibitor lorlatinib exhibited excellent inhibitory activities against wild-type ALK (ALK IC_{50} = 1.3 nmol/L) and clinical mutants (ALK-1196M IC_{50} = 21 nmol) and also had improved CNS penetration (MDR BA/AB = 1.5 *vs.* 45) as well as kinase selectivity.

The protein−protein interaction (PPI) between B-cell lymphoma 6 (BCL6) and its corepressors has been proposed as an attractive drug target for the treatment of diffuse large B-cell lymphoma (DLBCL) cancers[139]. In 2017, starting with a hit fragment **46** (Fig. 24, K_d = 689 μmol/L), McCoull et al.[140] discovered the macrocycle pyrazolo[1,5-*a*]pyrimidine BCL6 binder **47** (K_d = 0.0065 μmol/L) with 100,000-fold increased binding affinity through the structure-based drug design. The X-ray structure of **47** bound to BCL6 demonstrated that several hydrogen bonds were formed by the OH group with Y58, the pyrazole N atom with M51 as well as the lactam oxygen with E115, which were reinforced by the geometry of macrocyclic linker (PDB code: 5N1Z).

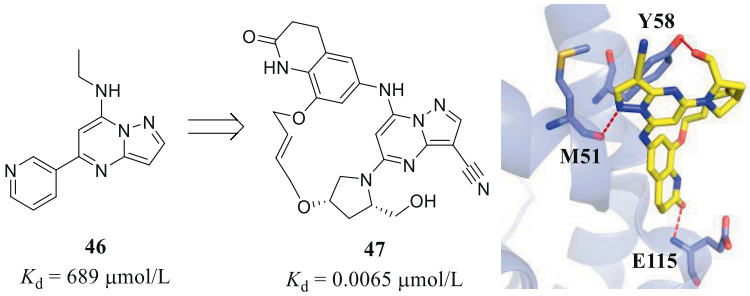

Figure 24 The discovery of the macrocyclic BCL6 inhibitor **47** (PDB code: 5N1Z). The inhibitor **47** is displayed in the yellow stick. The H-bonding interactions between **47** and the BCL6 protein matrix are indicated by the red dotted lines.

The epidermal growth factor receptor (EGFR) is a receptor tyrosine kinase that transduces mitogenic signals[141,142]. T790M and C797S mutations are two prevalent EGFR mutations in NSCLC tumors, which could cause ligand-independent EGFR activation and sensitize NSCLC tumors to EGFR tyrosine kinase inhibitors (TKIs)[143]. In 2019, Engelhardt et al.[144] identified the aminobenzimidazole **48** as a promising lead compound (Fig. 25), it demonstrated moderate binding affinity toward mutated EGFR ($EGFR^{del19/T790M/C797S}$ IC_{50} = 250 nmol/L) and no affinity to $EGFR^{WT}$ ($EGFR^{WT}$ IC_{50} > 100 μmol/L) as well as acceptable cellular activity (BaF3 cells IC_{50} = 300 nmol/L). From the co-crystal structure of **48** (PDB code: 6S9B), they also observed several H-bonding interactions between the carbonyl oxygen group of **48** and benzimidazole NH and M793, respectively, as well as the pyridine N atom with K745. The isobutyl hydroxy group filled the sugar pocket and formed H-bonding interaction with C797. Additionally, there was a two-point hinge binding between the two aromatic rings (~40°), which was proved to be a low-energy conformation and important for our further optimization. Similar to lorlatinib, the macrocyclization strategy was also successfully applied to the discovery of BI-4020 (**49**), a noncovalent EGFR inhibitor with excellent *in vitro* and *in vivo* inhibitory potency ($EGFR^{del19\ T790M\ C797S}$ IC_{50} = 0.6 nmol/L, BaF3 cells IC_{50} = 0.2 nmol/L). Furthermore, **49** displayed excellent kinase selectivity, while sparing ample $EGFR^{WT}$ ($EGFR^{WT}$ IC_{50} > 400 μmol/L).

Recently, Chen et al.[145] originally reported a series of 4-indolyl-2-phenylaminopyrimidine-based $EGFR^{C797S}$ inhibitors by hybridizing the scaffolds of approved drugs Osimertinib and Brigatinib, and the compound **50** exhibited excellent kinase inhibitory activities against $EGFR^{L858R/T790M/C797S}$ and $EGFR^{19del/T790M/C797S}$ with IC_{50} values of 4.3 and 25.6 nmol/L, respectively (Fig. 26). However, compound **50** had a poor cellular permeability, which caused the unsatisfied antiproliferative effect. The co-crystal structure of $EGFR^{T790M/C797S}$ with **50** showed that compound **50** adopted a "U-shape" conformation, and formed three hydrogen bonds between the N atom of pyrimidine with L792, the NH of aniline with the backbone carbonyl of M793 and the ethyl sulfonate moiety with K745. Importantly, it also revealed that there was a dihedral angle of −30.9° upon binding between the pyrimidine and the 4-(3-indolyl) group, which implied that the conformationally constrained macrocyclization strategy may be used to avoid the entropy-driven binding affinity loss. Further optimizations were carried out based on the structural information. Encouragingly, the macrocyclic compound **51** not only maintained comparable kinase inhibitory activity against $EGFR^{del19/T790M/C797S}$ (IC_{50} = 15.8 nmol/L) but also displayed a significantly improved

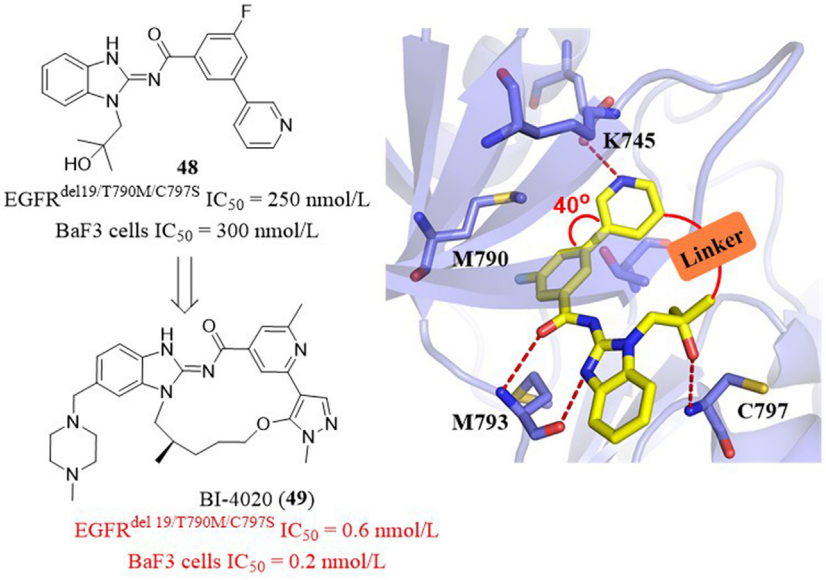

Figure 25 The discovery of the macrocyclic EGFR inhibitor **49**. The inhibitor **48** is displayed in the yellow stick. The H-bonding interactions between **48** and the EGFR protein are indicated by the red dotted lines (PDB code: 6S9B).

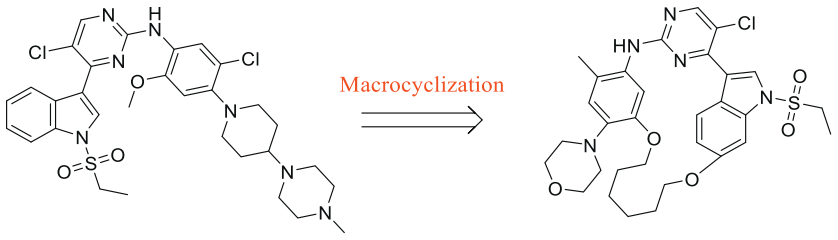

50
$EGFR^{del19/T790M/C797S}$ IC_{50} = 25.6 nmol/L
Ba/F3 cells IC_{50} = 3.156 μmol/L

51
$EGFR^{del19/T790M/C797S}$ IC_{50} = 15.8 nmol/L
Ba/F3 cells IC_{50} = 0.052 μmol/L

Figure 26 The discovery of the macrocyclic EGFR inhibitor **51**.

antiproliferative activity against Ba/F3 cells (IC_{50} = 0.052 μmol/L *vs.* 3.156 μmol/L). However, compound **51** exhibited unfavorable oral PK properties (F = 11.9%).

As the activated form of the zymogen factor XI (FXI), trypsin-like serine protease factor XIa (FXIa) plays an important role in the blood coagulation cascade and may contribute to thrombosis risk[146,147]. Pinto et al.[148] have disclosed the phenyl substituted imidazole **52** with excellent FXIa inhibitory activity (Fig. 27, K_i = 5.8 nmol/L) and moderate anticoagulant activity (aPTT $EC_{1.5x}$ = 5.3 μmol/L) in 2015. To further improve aPTT potency, they reported a series of novel macrocyclic FXIa inhibitors *via* linking the benzyl and phenyl groups of compound **52**. Among these inhibitors, the macrocycle **53** containing an *E*-alkene showed picomolar FXIa inhibitory activity (K_i = 0.03 nmol/L), improved aPTT potency ($EC_{1.5x}$ = 0.28 μmol/L) and over 1000-fold selectivity over other blood coagulation enzymes[149]. Although the macrocyclic amide linker formed a hydrogen bond with L41 and significantly contributed to the improved FXIa potency, it also had poor oral bioavailability (F = 1%).

Glutaminases (GLSs) including kidney-type glutaminase (GLS1) and liver-type glutaminase (GLS2) are key enzymes that catalyze glutamine to glutamate[150]. CB839 (Fig. 28) is a widely recognized allosteric inhibitor with an IC_{50} of 22 nmol/L, the previously published X-ray crystal structure revealed an U-shaped configuration with a distance of 10.58 Å between the terminal atoms (PDB code: 5HL1), which provided a certain chemical space allowing for the introduction of a macrocyclic linker[151,152]. Based on the structural information, Bian et al.[153] reported a series of macrocyclic GLS1 inhibitors by linking the terminal aromatic rings of CB839. The most promising compound **54** not only showed robust inhibitory activity in enzymatic and cellular levels (GLS1 IC_{50} = 6 nmol/L, HCT116 IC_{50} = 81 nmol/L), but also induced ROS activation by blocking glutamine metabolism. Compound **54** also exhibited comparable *in vivo* antitumor effects as CB839.

Mcl-1, a member of the anti-apoptotic protein Bcl-2 family, is a major component of the mitochondrial apoptotic pathway[154]. The Mcl-1 gene is amplified in a variety of human tumors, and the high expression of Mcl-1 is closely related to the development of resistance to chemotherapy[8]. In tumor cells, Mcl-1 and pro-apoptotic proteins (*e.g.*, Bak, Bid, Bad, etc.) exert anti-apoptotic effects through protein−protein interactions, leading to tumor cell proliferation. However, such PPI has a large contact interface and strong affinity, making the development of small-molecule drugs difficult[155].

The researchers from AstraZeneca found that compound **55** inhibited Mcl-1 with an IC_{50} of 0.042 μmol/L[156]. By analyzing the X-ray crystal structure (Fig. 29, PDB code: 6FS1), they found that **55** adopted an U-shaped configuration and occupied a larger hydrophobic space, its indole-2-carboxylic acid formed an ionic interaction with R263. Particularly, the distance between the pyrazole methyl group and the naphthalene ring was only 3.6 Å, allowing for subsequent structural modifications. They then designed several macrocyclic compounds by linking the pyrazole methyl of **55** to its naphthalene ring. As expected, (R_a)-6-Cl indole derivative AZD5991 (**56**) exhibited significantly improved inhibitory activity (IC_{50} = 0.7 nmol/L) and complete tumor regression (TGI = 100%) in the multiple myeloma model and acute myeloid leukemia model. Currently, the compound is undergoing phase II clinical evaluation for the treatment of acute myeloid leukemia (ClinicalTrials.gov identifier: NCT03218683 and NCT03013998).

The proteolysis targeting chimeras (PROTAC) molecules are bifunctional molecules by recruiting cellular degradation machinery to induce ubiquitination and subsequent proteasomal degradation[103,157,158]. McCoull et al.[159] first developed a macrocycle-based therapeutic modality combined with PROTAC technology for the development of BCL6 modulators in 2018. They originally

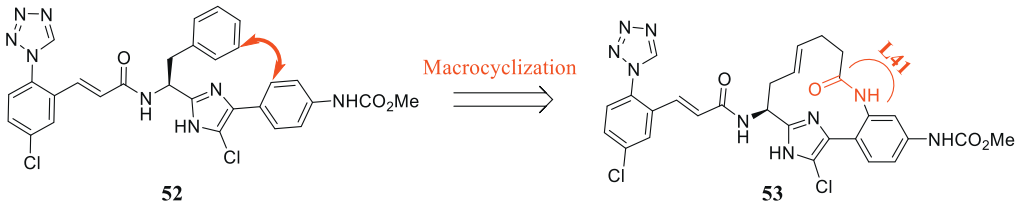

52
FXIa K_i = 5.8 nmol/L
aPTT $EC_{1.5x}$ = 5.3 μmol/L

53
FXIa K_i = 0.03 nmol/L
aPTT $EC_{1.5x}$ = 0.28 μmol/L

Figure 27 The discovery of the macrocyclic FXIa inhibitor **53**.

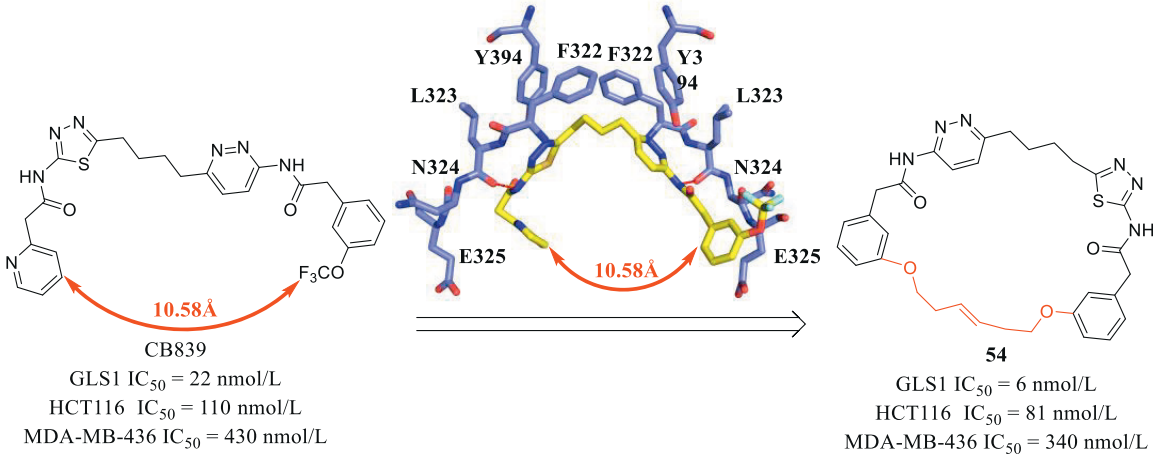

Figure 28 Discovery of the macrocyclic GLS1 inhibitor **54**. The inhibitor CB839 is displayed in the yellow stick (PDB code: 5HL1).

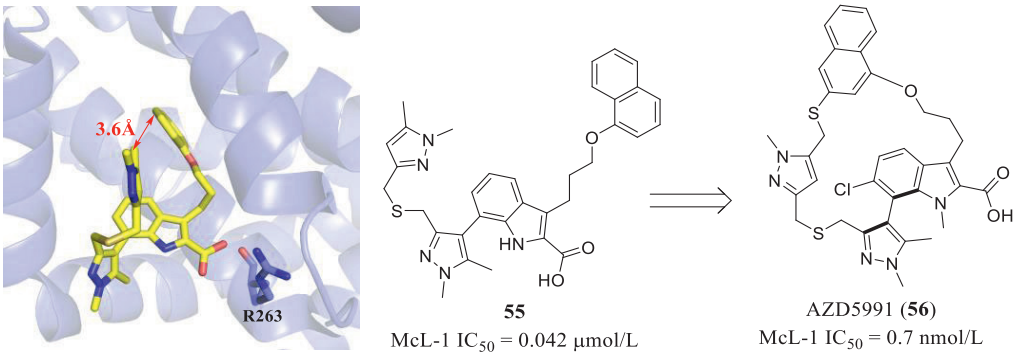

Figure 29 The discovery of the macrocyclic Mcl-1 specific inhibitor AZD5991. The inhibitor **56** is displayed in the yellow stick (PDB code: 6FS1).

obtained the macrocycle inhibitor **58** by pursuing a hit-to-lead optimization campaign of hit **57**, which demonstrated excellent inhibitory activity against BCL6 (IC_{50} = 0.0089 μmol/L, Fig. 30). Nextly, the macrocycle-based PROTAC **59** was designed through the conjugation of **58** with the CRBN binder thalidomide. Although **59** could effectively degrade BCL-6 in a dose-dependent fashion (82% degradation at 1 μmol/L), it did not show a significant anti-proliferative effect and phenotypic response.

In 2019, Testa et al.[160] reported the first BET macrocyclic PROTAC molecule **60** ($BRD4^{BD2}$ K_d = 15 nmol/L, Fig. 31) by introducing an ether linker to the BET degrader MZ1[160]. The X-ray co−crystal structure of MZ1 (PDB code: 5T35)[161,162] revealed that MZ1 adopted an U-shaped configuration, and its two ligand moieties laid in close spatial proximity with a distance of 7.9 Å. Based on this structural information, they designed a macrocyclic PROTAC by adding an ether linker to lock the PROTAC configuration. Encouragingly, the corresponding MacroPROTAC-1 (**60**) exhibited high binary binding affinity ($BRD4^{BD2}$ K_d = 180 nmol/L, VHL K_i = 33 nmol/L) and comparable cellular degradation activity to MZ1 (DC_{50} < 125 nmol/L). Furthermore, compound **60**

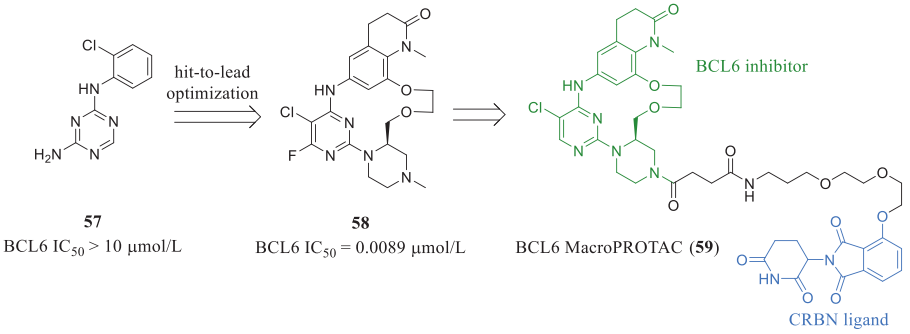

Figure 30 Discovery of the BCL6 macrocyclic PROTAC **59**.

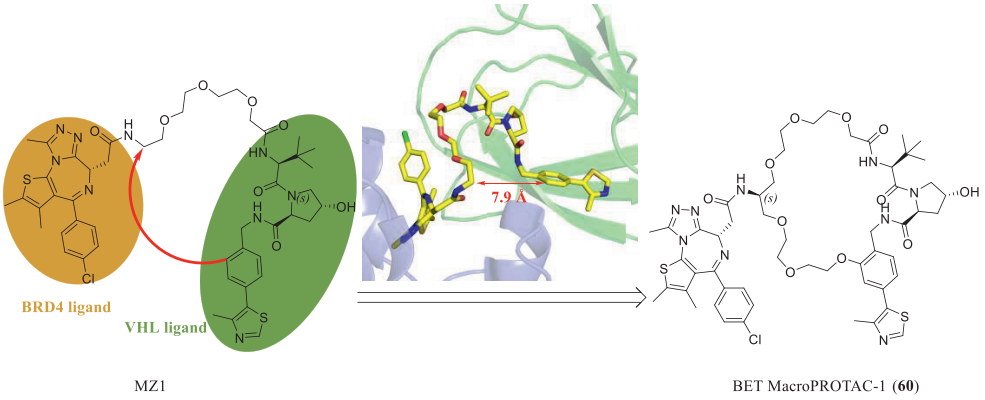

Figure 31 Discovery of the first BET macrocyclic PROTAC **60**. The PROTAC MZ1 is displayed in the yellow stick (PDB code: 5T35).

also showed good antiproliferative activity in 22RV1 cells (EC_{50} = 640 nmol/L) and MV4; 11 cells (EC_{50} = 300 nmol/L). These findings support that macrocyclic PROTACs may represent an alternative strategy for the development of new PROTAC degraders.

3. Conclusions and perspectives

The design of highly potent and specific ligands for the targets of interest has been a continued challenge in recent years. As one of the most commonly applied methods in drug discovery, the cyclization strategy has proven to significantly increase the binding affinity and selectivity *via* stabilizing the binding pattern. Moreover, due to the scaffold change and increased structural novelty of cyclized compounds, this strategy could provide feasible ways to discover new lead compounds based on the patented compounds. The cyclization strategy has been successfully applied to the discovery of novel drug candidates for treating various diseases, some drugs including Dolutegravir have been approved by the FDA.

When designing new cyclized compounds based on existing leading compounds, the newly cyclized scaffold should maintain original key interactions with the targets of interest, the modifiable sites for cyclization should be solvent exposed or do not have key interactions with the proteins of interest. However, there are still several challenges facing the researchers, including (i) the synthetic intractability limits further investigation of the cyclized compounds, particularly for macrocycles. In addition, the development of novel synthetic methods may facilitate the macrocycle-based drug discovery; (ii) the macrocycles are structurally complex and have high molecular weight, thus showing relatively poor PK profiles; (iii) for some proteins, the structural information of the small molecule/protein complexes are rarely reported, making structure-based cyclization less rationale and more challenging. Anyway, we believe the cyclization strategy will find wide applications in drug discovery.

Acknowledgments

This work is supported by the National Natural Science Foundation of China (Nos. 22277110, 81973177 and 31900875, China), the Natural Science Foundation of Henan Province (Nos. 222300420069 and 222301420049, China), and Program for Science & Technology Innovation Talents in Universities of Henan Province (No. 21HASTIT045, China).

Author contributions

Bin Yu conceived this project, revised this review extensively, and submitted this review on behalf of other authors. Bin Yu, Kai Tang, Yihui Song, Shu Wang and Wenshuo Gao wrote this review together.

Conflicts of interest

The authors have no conflicts of interest to declare.

References

1. Deore AB, Dhumane JR, Wagh HV, Sonawane RB. The stages of drug discovery and development process. *Asian J Pharm Res Dev* 2019;**7**:62–7.
2. Lakshmana Prabu S, Thirumurugan R. Lead optimization in the drug discovery process. In: Puratchikody A, Prabu SL, Umamaheswari A, editors. *Computer appliciations in drug discovery and development*. 3rd ed. Hershey, PA: IGI Global; 2019. p. 62–79.
3. Sean RC, Xuan F, Ellen EC, Marsha PP, Jaroslava S, Jordan RB, et al. Inhibitory and stimulatory micropeptides preferentially bind to different conformations of the cardiac calcium pump. *J Biol Chem* 2022;**298**:102060.
4. Zhao H, Guo Z. Medicinal chemistry strategies in follow-on drug discovery. *Drug Discov Today* 2009;**14**:516–22.
5. Fang Z, Song Y, Zhan P, Zhang Q, Liu X. Conformational restriction: an effective tactic in follow-on-based drug discovery. *Future Med Chem* 2014;**6**:885–901.
6. Zheng Y, Tice CM, Singh SB. Conformational control in structure-based drug design. *Bioorg Med Chem Lett* 2017;**27**:2825–37.
7. Chen F, Jane PC. Molecular energy levels. In: Chen F, Jane PC, editors. *Lecture notes on principles of plasma processing*. 4th ed. Boston: Springer; 2003. p. 137–9.
8. Soustelle M. *Molecular partition functions. Phase modeling tools*. 5th ed. London: ISTE Ltd.; 2015. p. 131–67.
9. Verteramo ML, Stenström O, Ignjatović MM, Caldararu O, Olsson MA, Manzoni F, et al. Interplay between conformational entropy and solvation entropy in protein–ligand binding. *J Am Chem Soc* 2019;**6**:2012–26.
10. Williams DH, Stephens E, O'Brien DP, Zhou M. Understanding noncovalent interactions: ligand binding energy and catalytic efficiency from ligand-induced reductions in motion within receptors and enzymes. *Angew Chem Int Ed* 2004;**10**:6596–616.
11. Sampson PB, Liu Y, Forrest B, Cumming G, Li SW, Patel NK, et al. The discovery of polo-like kinase 4 inhibitors: identification of (1*R*,2*S*)-2-(3-((*E*)-4-(((*cis*)2,6-dimethylmorpholino)methyl)styryl)-1*H*-indazol-6-yl)-5′-methoxyspiro[cyclopropane-1,3′-indolin]-2′-one

(CFI-400945) as a potent, orally active antitumor agent. *J Med Chem* 2015;**58**:147−69.
12. Yu B, Yu Z, Qi PP, Yu DQ, Liu HM. Discovery of orally active anticancer candidate CFI-400945 derived from biologically promising spirooxindoles: success and challenges. *Eur J Med Chem* 2015;**95**:35−40.
13. O'Reilly MC, Scott SA, Brown KA, Oguin 3rd TH, Thomas PG, Daniels JS, et al. Development of dual PLD1/2 and PLD2 selective inhibitors from a common 1,3,8-triazaspiro[4.5]decane core: discovery of Ml298 and Ml299 that decrease invasive migration in U87-MG glioblastoma cells. *J Med Chem* 2013;**56**:2695−9.
14. Tron GC, Pirali T, Sorba G, Pagliai F, Busacca S, Genazzani AA. Medicinal chemistry of combretastatin A4: present and future directions. *J Med Chem* 2006;**49**:3033−44.
15. Andersson H, Demaegdt H, Vauquelin G, Lindeberg G, Karlen A, Hallberg M, et al. Disulfide cyclized tripeptide analogues of angiotensin IV as potent and selective inhibitors of insulin-regulated aminopeptidase (IRAP). *J Med Chem* 2010;**53**:8059−71.
16. Davies JS. The cyclization of peptides and depsipeptides. *J Pept Sci* 2003;**9**:471−501.
17. Fang Y, Yang C, Yu Z, Li X, Mu Q, Liao G, et al. Natural products as LSD1 inhibitors for cancer therapy. *Acta Pharm Sin B* 2021;**11**:621−31.
18. Gao Y, Voigt J, Wu JX, Yang D, Burke JTR. Macrocyclization in the design of a conformationally constrained Grb2 SH2 domain inhibitor. *Bioorg Med Chem Lett* 2001;**11**:1889−92.
19. Gao Y, Wei C, Fau-Burke Jr TR, Burke Jr TR. Olefin metathesis in the design and synthesis of a globally constrained Grb2 SH2 domain inhibitor. *Org Lett* 2001;**3**:1617−20.
20. Meyer JH, Bartlett PA. Macrocyclic inhibitors of penicillopepsin 1 design, synthesis, and evaluation of an inhibitor bridged between P1 and P3. *J Am Chem Soc* 1998;**120**:4600−9.
21. Miller SJ, Blackwell HE, Grubbs RH. Application of ring-closing metathesis to the synthesis of rigidified amino acids and peptides. *J Am Chem Soc* 1996;**118**:9606−14.
22. Mollica A, Pinnen F, Stefanucci A, Feliciani F, Campestre C, Mannina L, et al. The *cis*-4-amino-l-proline residue as a scaffold for the synthesis of cyclic and linear endomorphin-2 analogues. *J Med Chem* 2012;**55**:3027−35.
23. Schmidt M, Toplak A, Quaedflieg P, van Maarseveen JH, Nuijens T. Enzyme-catalyzed peptide cyclization. *Drug Discov Today Technol* 2017;**26**:11−6.
24. Tal-Gan Y, Hurevich M, Klein S, Ben-Shimon A, Rosenthal D, Hazan C, et al. Backbone cyclic peptide inhibitors of protein kinase B (PKB/Akt). *J Med Chem* 2011;**54**:5154−64.
25. Thakkar A, Trinh TB, Pei D. Global analysis of peptide cyclization efficiency. *ACS Comb Sci* 2013;**15**:120−9.
26. Xu S, Li H, Shao X, Fan C, Ericksen B, Liu J, et al. Critical effect of peptide cyclization on the potency of peptide inhibitors against Dengue virus NS2B-NS3 protease. *J Med Chem* 2012;**55**:6881−7.
27. Chang RQ, Li DJ, Li MQ. The role of indoleamine-2,3-dioxygenase in normal and pathological pregnancies. *Am J Reprod Immunol* 2018;**79**:e12786.
28. Mellor AL, Chandler P, Lee GK, Johnson T, Keskin DB, Lee J, et al. Indoleamine 2,3-dioxygenase, immunosuppression and pregnancy. *J Reprod Immunol* 2002;**57**:143−50.
29. Tang K, Wang B, Yu B, Liu HM. Indoleamine 2,3-dioxygenase 1 (Ido1) inhibitors and PROTAC-based degraders for cancer therapy. *Eur J Med Chem* 2022;**227**:113967.
30. Tang K, Wu YH, Song Y, Yu B. Indoleamine 2,3-dioxygenase 1 (Ido1) inhibitors in clinical trials for cancer immunotherapy. *J Hematol Oncol* 2021;**14**:68.
31. Kumar S, Waldo JP, Jaipuri FA, Marcinowicz A, Van Allen C, Adams J, et al. Discovery of clinical candidate (1*R*,4*R*)-4-((*R*)-2-((*S*)-6-fluoro-5*H*-imidazo[5,1-*a*]isoindol-5-yl)-1-hydroxyethyl)cyclohexan-1-ol(navoximod), a potent and selective inhibitor of indoleamine 2,3-dioxygenase 1. *J Med Chem* 2019;**62**:6705−33.
32. Zhang H, Liu K, Pu Q, Achab A, Ardolino MJ, Cheng M, et al. Discovery of amino-cyclobutarene-derived indoleamine-2,3-dioxygenase 1 (Ido1) Inhibitors for cancer immunotherapy. *ACS Med Chem Lett* 2019;**10**:1530−6.
33. Cheng MF, Hung MS, Song JS, Lin SY, Liao FY, Wu MH, et al. Discovery and structure−activity relationships of phenyl benzenesulfonylhydrazides as novel indoleamine 2,3-dioxygenase inhibitors. *Bioorg Med Chem Lett* 2014;**24**:3403−6.
34. Lin SY, Yeh TK, Kuo CC, Song JS, Cheng MF, Liao FY, et al. Phenyl benzenesulfonylhydrazides exhibit selective indoleamine 2,3-dioxygenase inhibition with potent *in vivo* pharmacodynamic activity and antitumor efficacy. *J Med Chem* 2016;**59**:419−30.
35. Agboyibor C, Dong J, Effah CY, Drokow EK, Pervaiz W, Liu HM. LSD1 as a biomarker and the outcome of its inhibitors in the clinical trial: the therapy opportunity in tumor. *J Oncol* 2021;**2021**:5512524.
36. Fu X, Zhang P, Yu B. Advances toward LSD1 inhibitors for cancer therapy. *Future Med Chem* 2017;**9**:1227−42.
37. Gu F, Lin Y, Wang Z, Wu X, Ye Z, Wang Y, et al. Biological roles of LSD1 beyond its demethylase activity. *Cell Mol Life Sci* 2020;**77**:3341−50.
38. Karakaidos P, Verigos J, Magklara A. LSD1/KDM1A, a gate-keeper of cancer stemness and a promising therapeutic target. *Cancers* 2019;**11**:1821.
39. Dai XJ, Liu Y, Xiong XP, Xue LP, Zheng YC, Liu HM. Tranylcypromine based lysine-specific demethylase 1 inhibitor: summary and perspective. *J Med Chem* 2020;**63**:14197−215.
40. Fang Y, Liao G, Yu B. LSD1/KDM1A inhibitors in clinical trials: advances and prospects. *J Hematol Oncol* 2019;**12**:129.
41. Ji YY, Lin SD, Wang YJ, Su MB, Zhang W, Gunosewoyo H, et al. Tying up tranylcypromine: novel selective histone lysine specific demethylase 1 (LSD1) inhibitors. *Eur J Med Chem* 2017;**141**:101−12.
42. Li C, Su M, Zhu W, Kan W, Ge T, Xu G, et al. Structure−activity relationship study of indolin-5-yl-cyclopropanamine derivatives as selective lysine specific demethylase 1 (LSD1) inhibitors. *J Med Chem* 2022;**65**:4335−49.
43. Dai XJ, Liu Y, Xue LP, Xiong XP, Zhou Y, Zheng YC, et al. Reversible lysine specific demethylase 1 (LSD1) inhibitors: a promising wrench to impair LSD1. *J Med Chem* 2021;**64**:2466−88.
44. Sorna V, Theisen ER, Stephens B, Warner SL, Bearss DJ, Vankayalapati H, et al. High-throughput virtual screening identifies novel *N′*-(1-phenylethylidene)-benzohydrazides as potent, specific, and reversible LSD1 inhibitors. *J Med Chem* 2013;**56**:9496−508.
45. Zhou Y, Li Y, Wang WJ, Xiang P, Luo XM, Yang L, et al. Synthesis and biological evaluation of novel (*E*)-*N′*-(2,3-dihydro-1*H*-inden-1-ylidene) benzohydrazides as potent LSD1 inhibitors. *Bioorg Med Chem Lett* 2016;**26**:4552−7.
46. Wang X, Zhang C, Zhang X, Yan J, Wang J, Jiang Q, et al. Design, synthesis and biological evaluation of tetrahydroquinoline-based reversible LSD1 inhibitors. *Eur J Med Chem* 2020;**194**:112243.
47. Zhang X, Huang H, Zhang Z, Yan J, Wu T, Yin W, et al. Design, synthesis and biological evaluation of novel benzofuran derivatives as potent LSD1 inhibitors. *Eur J Med Chem* 2021;**220**:113501.
48. Falkenberg KJ, Johnstone RW. Histone deacetylases and their inhibitors in cancer, neurological diseases and immune disorders. *Nat Rev Drug Discov* 2014;**13**:673−91.
49. Gallinari P, Di Marco S, Jones P, Pallaoro M, Steinkühler C. HDACs, histone deacetylation and gene transcription: from molecular biology to cancer therapeutics. *Cell Res* 2007;**17**:195−211.
50. Sambucetti LC, Fischer DD, Zabludoff S, Kwon PO, Chamberlin H, Trogani N, et al. Histone deacetylase inhibition selectively alters the activity and expression of cell cycle proteins leading to specific chromatin acetylation and antiproliferative effects. *J Biol Chem* 1999;**274**:34940−7.
51. Zhang XH, Qin M, Wu HP, Khamis MY, Li YH, Ma LY, et al. A review of progress in histone deacetylase 6 inhibitors research: structural specificity and functional diversity. *J Med Chem* 2021;**64**:1362−91.

52. Taha TY, Aboukhatwa SM, Knopp RC, Ikegaki N, Abdelkarim H, Neerasa J, et al. Design, synthesis, and biological evaluation of tetrahydroisoquinoline-based histone deacetylase 8 selective inhibitors. *ACS Med Chem Lett* 2017;**8**:824−9.
53. McClure JJ, Zhang C, Inks ES, Peterson YK, Li J, Chou CJ. Development of allosteric hydrazide-containing class I histone deacetylase inhibitors for use in acute myeloid leukemia. *J Med Chem* 2016;**59**:9942−59.
54. Jiang Y, Xu J, Yue K, Huang C, Qin M, Chi D, et al. Potent hydrazide-based HDAC inhibitors with a superior pharmacokinetic profile for efficient treatment of acute myeloid leukemia *in vivo*. *J Med Chem* 2022;**65**:285−302.
55. Hendriks RW, Yuvaraj S, Kil LP. Targeting bruton's tyrosine kinase in B cell malignancies. *Nat Rev Cancer* 2014;**14**:219−32.
56. Kurosaki T. Functional dissection of BCR signaling pathways. *Curr Opin Immunol* 2000;**12**:276−81.
57. Pal Singh S, Dammeijer F, Hendriks RW. Role of bruton's tyrosine kinase in B cells and malignancies. *Mol Cancer* 2018;**17**:57.
58. Satterthwaite AB, Witte ON. The role of bruton's tyrosine kinase in B-cell development and function: a genetic perspective. *Immunol Rev* 2000;**175**:120−7.
59. Guo Y, Liu Y, Hu N, Yu D, Zhou C, Shi G, et al. Discovery of zanubrutinib (BGB-3111), a novel, potent, and selective covalent inhibitor of bruton's tyrosine kinase. *J Med Chem* 2019;**62**:7923−40.
60. Pan Z, Scheerens H, Li SJ, Schultz BE, Sprengeler PA, Burrill LC, et al. Discovery of selective irreversible inhibitors for bruton's tyrosine kinase. *ChemMedChem* 2007;**2**:58−61.
61. Bender AT, Gardberg A, Pereira A, Johnson T, Wu Y, Grenningloh R, et al. Ability of bruton's tyrosine kinase inhibitors to sequester Y551 and prevent phosphorylation determines potency for inhibition of fc receptor but not B-cell receptor signaling. *Mol Pharmacol* 2017;**91**:208−19.
62. Xue Y, Song P, Song Z, Wang A, Tong L, Geng M, et al. Discovery of 4,7-diamino-5-(4-phenoxyphenyl)-6-methylene-pyrimido[5,4-*b*]pyrrolizines as novel bruton's tyrosine kinase inhibitors. *J Med Chem* 2018;**61**:4608−27.
63. Kawahata WAO, Asami T, Kiyoi T, Irie T, Taniguchi H, Asamitsu Y, et al. Design and synthesis of novel amino-triazine analogues as selective bruton's tyrosine kinase inhibitors for treatment of rheumatoid arthritis. *J Med Chem* 2018;**61**:8917−33.
64. Cheng Y, Ma XL, Wei YQ, Wei XW. Potential roles and targeted therapy of the CXCLs/CXCR2 axis in cancer and inflammatory diseases. *Biochim Biophys Acta Rev Cancer* 2019;**187**:289−312.
65. Busch-Petersen J, Wang Y. Phenol-containing antagonists of the CXCR2 receptor. *Expert Opin Ther Pat* 2008;**18**:629−37.
66. Dong Y, Fu R, Chen J, Zhang K, Ji M, Wang M, et al. Discovery of benzocyclic sulfone derivatives as potent CXCR2 antagonists for cancer immunotherapy. *J Med Chem* 2021;**64**:16626−40.
67. Abbracchio MP, Burnstock G, Boeynaems JM, Barnard EA, Boyer JL, Kennedy C, et al. International union of pharmacology LVIII: update on the P2Y G protein-coupled nucleotide receptors: from molecular mechanisms and pathophysiology to therapy. *Pharmacol Rev* 2006;**58**:281−341.
68. Dorsam RT, Kunapuli SP. Central role of the P2Y12 receptor in platelet activation. *J Clin Invest* 2004;**113**:340−5.
69. Bach P, Antonsson T, Bylund R, Björkman JA, Österlund K, Giordanetto F, et al. Lead optimization of ethyl 6-aminonicotinate acyl sulfonamides as antagonists of the P2Y12 receptor. separation of the antithrombotic effect and bleeding for candidate drug AZD1283. *J Med Chem* 2013;**56**:7015−24.
70. Kong D, Xue T, Guo B, Cheng J, Liu S, Wei J, et al. Optimization of P2Y12 antagonist ethyl 6-(4-((benzylsulfonyl)carbamoyl)piperidin-1-yl)-5-cyano-2-methylnicotinate (AZD1283) led to the discovery of an oral antiplatelet agent with improved druglike properties. *J Med Chem* 2019;**62**:3088−106.
71. Masuda M, Uno Y, Ohbayashi N, Ohata H, Mimata A, Kukimoto-Niino M, et al. TNIK inhibition abrogates colorectal cancer stemness. *Nat Commun* 2016;**7**:12586.
72. Satow R, Shitashige M, Jigami T, Honda K, Ono M, Hirohashi S, et al. TRAF2- and NCK-interacting kinase is essential for canonical WNT signaling in xenopus axis formation. *J Biol Chem* 2010;**285**:26289−94.
73. Takahashi H, Ishikawa T, Ishiguro M, Okazaki S, Mogushi K, Kobayashi H, et al. Prognostic significance of TRAF2- and NCK-interacting kinase (TNIK) in colorectal cancer. *BMC Cancer* 2015;**15**:794.
74. Li Y, Zhang L, Yang R, Qiao Z, Wu M, Huang C, et al. Discovery of 3,4-dihydrobenzo[*f*][1,4]oxazepin-5(2*H*)-one derivatives as a new class of selective TNIK inhibitors and evaluation of their anti-colorectal cancer effects. *J Med Chem* 2022;**65**:1786−807.
75. McLean GW, Carragher NO, Avizienyte E, Evans J, Brunton VG, Frame MC. The role of focal-adhesion kinase in cancer—a new therapeutic opportunity. *Nat Rev Cancer* 2005;**5**:505−15.
76. Hospital MA, Green AS, Maciel TT, Moura IC, Leung AY, Bouscary D, et al. FLT3 inhibitors: clinical potential in acute myeloid leukemia. *OncoTargets Ther* 2017;**10**:607−15.
77. Carter BZ, Mak PY, Wang X, Yang H, Garcia-Manero G, Mak DH, et al. Focal adhesion kinase as a potential target in AML and MDS. *Mol Cancer Ther* 2017;**16**:1133−44.
78. Recher C, Ysebaert L, Beyne-Rauzy O, Mansat-De Mas V, Ruidavets JB, Cariven P, et al. Expression of focal adhesion kinase in acute myeloid leukemia is associated with enhanced blast migration, increased cellularity, and poor prognosis. *Cancer Res* 2004;**64**:3191−7.
79. Cho H, Shin I, Yoon H, Jeon E, Lee J, Kim Y, et al. Identification of thieno[3,2-*d*]pyrimidine derivatives as dual inhibitors of focal adhesion kinase and FMS-like tyrosine kinase 3. *J Med Chem* 2021;**64**:11934−57.
80. Margueron R, Reinberg D. The polycomb complex PRC2 and its mark in life. *Nature* 2011;**469**:343−9.
81. McCabe MT, Graves AP, Ganji G, Diaz E, Halsey WS, Jiang Y, et al. Mutation of A677 in histone methyltransferase EZH2 in human B-cell lymphoma promotes hypertrimethylation of histone H3 on lysine 27 (H3K27). *Proc Natl Acad Sci U S A* 2012;**109**:2989−94.
82. Sneeringer CJ, Scott MP, Kuntz KW, Knutson SK, Pollock RM, Richon VM, et al. Coordinated activities of wild-type plus mutant EZH2 drive tumor-associated hypertrimethylation of lysine 27 on histone H3 (H3K27) in human B-cell lymphomas. *Proc Natl Acad Sci U S A* 2010;**107**:20980−5.
83. Kung PP, Rui E, Bergqvist S, Bingham P, Braganza J, Collins M, et al. Design and synthesis of pyridone-containing 3,4-dihydroisoquinoline-1(2*H*)-ones as a novel class of enhancer of zeste homolog 2 (EZH2) inhibitors. *J Med Chem* 2016;**59**:8306−25.
84. Cheng X, Kinosaki MM, Takami MY, Choi H, Zhang R, Murali R. Disabling of receptor activator of nuclear factor-kappaB (RANK) receptor complex by novel osteoprotegerin-like peptidomimetics restores bone loss *in vivo*. *J Biol Chem* 2004;**279**:8269−77.
85. Nakashima T, Hayashi MT, Fukunaga TK, Kurata KM, Oh-Hora MQ, Feng JF, et al. Evidence for osteocyte regulation of bone homeostasis through RANKL expression. *Nat Med* 2011;**17**:1231−4.
86. Tanaka S, Nakamura KN, Takahasi NT, Suda T. Role of RANKL in physiological and pathological bone resorption and therapeutics targeting the RANKL−RANK signaling system. *Immunol Rev* 2005;**208**:30−49.
87. Jiang M, Peng L, Yang K, Wang T, Yan X, Jiang T, et al. Development of small-molecules targeting receptor activator of nuclear factor-κB ligand (RANKL)-receptor activator of nuclear factor-κB (RANK) protein−protein interaction by structure-based virtual screening and hit optimization. *J Med Chem* 2019;**62**:5370−81.
88. Yang K, Li S, Wang T, Yan X, He Q, Ning R, et al. Development of an orally active small-molecule inhibitor of receptor activator of nuclear factor-kappaB ligand. *J Med Chem* 2022;**65**:10992−1009.
89. Taylor C, Gardier RW, Stoelting VK, Dallas ME. Clinical investigation of a new phenothiazine compound, methdilazine. *Clin Pharmacol Ther* 1962;**3**:593−8.

90. Boyd-Kimball D, Gonczy K, Lewis B, Mason T, Siliko N, Wolfe J. Classics in chemical neuroscience: chlorpromazine. *ACS Chem Neurosci* 2019;**10**:79−88.
91. Dong M, Ning ZQ, Xing PY, Xu JL, Cao HX, Dou GF, et al. Phase I study of chidamide (CS055/HBI-8000), a new histone deacetylase inhibitor, in patients with advanced solid tumors and lymphomas. *Cancer Chemother Pharmacol* 2012;**69**:1413−22.
92. Cui H, Hong Q, Wei R, Li H, Wan C, Chen X, et al. Design and synthesis of HDAC inhibitors to enhance the therapeutic effect of diffuse large B-cell lymphoma by improving metabolic stability and pharmacokinetic characteristics. *Eur J Med Chem* 2022;**229**:114049.
93. Bena S, Brancaleone V, Wang JM, Perretti M, Flower RJ. Annexin A1 interaction with the FPR2/ALX receptor: identification of distinct domains and downstream associated signaling. *J Biol Chem* 2012;**287**:24690−7.
94. Cattaneo F, Parisi M, Ammendola R. Distinct signaling cascades elicited by different formyl peptide receptor 2 (FPR2) agonists. *Int J Mol Sci* 2013;**14**:7193−230.
95. Corminboeuf O, Leroy X. FPR2/ALXR agonists and the resolution of inflammation. *J Med Chem* 2015;**58**:537−59.
96. Asahina Y, Wurtz NR, Arakawa K, Carson N, Fujii K, Fukuchi K, et al. Discovery of BMS-986235/LAR-1219: a potent formyl peptide receptor 2 (FPR2) selective agonist for the prevention of heart failure. *J Med Chem* 2020;**63**:9003−19.
97. Lassen A, Atefi M, Robert L, Wong DJ, Cerniglia M, Comin-Anduix B, et al. Effects of AKT inhibitor therapy in response and resistance to BRAF inhibition in melanoma. *Mol Cancer* 2014;**13**:83.
98. Testa JR, Bellacosa A. AKT plays a central role in tumorigenesis. *Proc Natl Acad Sci U S A* 2001;**98**:10983−5.
99. Xue G, Zippelius A, Wicki A, Mandalà M, Tang F, Massi D, et al. Integrated Akt/PKB signaling in immunomodulation and its potential role in cancer immunotherapy. *J Natl Cancer Inst* 2015;**107**:djv171.
100. Dumble M, Crouthamel MC, Zhang SY, Schaber M, Levy D, Robell K, et al. Discovery of novel AKT inhibitors with enhanced anti-tumor effects in combination with the MEK inhibitor. *PLoS One* 2014;**9**:e100880.
101. Dong X, Zhan W, Zhao M, Che J, Dai X, Wu Y, et al. Discovery of 3,4,6-trisubstituted piperidine derivatives as orally active, low hERG blocking Akt inhibitors *via* conformational restriction and structure-based design. *J Med Chem* 2019;**62**:7264−88.
102. Hiesinger K, Dar'in D, Proschak E, Krasavin M. Spirocyclic scaffolds in medicinal chemistry. *J Med Chem* 2021;**64**:150−83.
103. Fang Y, Liao G, Yu B. Small-molecule MDM2/X inhibitors and PROTAC degraders for cancer therapy: advances and perspectives. *Acta Pharm Sin B* 2020;**10**:1253−78.
104. Veber DF, Johnson SR, Cheng HY, Smith BR, Ward KW, Kopple KD. Molecular properties that influence the oral bioavailability of drug candidates. *J Med Chem* 2002;**45**:2615−23.
105. Lovering F, Bikker J, Humblet C. Escape from flatland: increasing saturation as an approach to improving clinical success. *J Med Chem* 2009;**52**:6752−6.
106. Hu Z, Fan C, Oh DS, Marron JS, He X, Qaqish BF, et al. The molecular portraits of breast tumors are conserved across microarray platforms. *BMC Genom* 2006;**7**:96.
107. Miller LD, Smeds J, George J, Vega VB, Vergara L, Ploner A, et al. An expression signature for p53 status in human breast cancer predicts mutation status, transcriptional effects, and patient survival. *Proc Natl Acad Sci U S A* 2005;**102**:13550−5.
108. van de Vijver MJ, He YD, van't Veer LJ, Dai H, Hart AA, Voskuil DW, et al. A gene-expression signature as a predictor of survival in breast cancer. *N Engl J Med* 2002;**347**:1999−2009.
109. Laufer R, Forrest B, Li SW, Liu Y, Sampson P, Edwards L, et al. The discovery of PLK4 inhibitors: (*E*)-3-((1*H*-indazol-6-yl)methylene) indolin-2-ones as novel antiproliferative agents. *J Med Chem* 2013;**56**:6069−87.
110. Barkowski R, Frishman W. HDL metabolism and CETP inhibition. *Cardiol Rev* 2008;**16**:154−62.
111. Heinz D. Reducing risk by raising HDL-cholesterol: the evidence. *Eur Heart J* 2006;**8**:23−9.
112. Tall AR, Yvan-Charvet L, Terasaka N, Pagler T, Wang N. HDL, ABC transporters, and cholesterol efflux: implications for the treatment of atherosclerosis. *Cell Metab* 2008;**7**:365−75.
113. Meanwell NA. Improving drug candidates by design: a focus on physicochemical properties as a means of improving compound disposition and safety. *Chem Res Toxicol* 2011;**24**:1420−56.
114. Peters JU, Schnider P, Mattei P, Kansy M. Pharmacological promiscuity: dependence on compound properties and target specificity in a set of recent roche compounds. *ChemMedChem* 2009;**4**:680−6.
115. Tarcsay Á, Keserű GM. Contributions of molecular properties to drug promiscuity. *J Med Chem* 2013;**56**:1789−95.
116. Schmeck C, Gielen-Haertwig H, Vakalopoulos A, Bischoff H, Li V, Wirtz G, Weber O. Novel tetrahydrochinoline derived CETP inhibitors. *Bioorg Med Chem Lett* 2010;**20**:1740−3.
117. Trieselmann T, Wagner H, Fuchs K, Hamprecht D, Berta D, Cremonesi P, et al. Potent cholesteryl ester transfer protein inhibitors of reduced lipophilicity: 1,1′-spiro-substituted hexahydrofuroquinoline derivatives. *J Med Chem* 2014;**57**:8766−76.
118. Song Y, Wang S, Zhao M, Yang Yu, B. Strategies targeting protein tyrosine phosphatase SHP2 for cancer therapy. *J Med Chem* 2022;**65**:3066−79.
119. Song Y, Yang X, Wang S, Zhao M, Yu B. Crystallographic landscape of SHP2 provides molecular insights for SHP2 targeted drug discovery. *Med Res Rev* 2022;**42**:1781−821.
120. Song Y, Zhao M, Zhang H, Yu B. Double-edged roles of protein tyrosine phosphatase SHP2 in cancer and its inhibitors in clinical trials. *Pharmacol Ther* 2022;**230**:107966.
121. Song Z, Wang M, Ge Y, Chen XP, Xu Z, Sun Y, et al. Tyrosine phosphatase SHP2 inhibitors in tumor-targeted therapies. *Acta Pharm Sin B* 2021;**11**:13−29.
122. Tang K, Jia YN, Yu B, Liu HM. Medicinal chemistry strategies for the development of protein tyrosine phosphatase SHP2 inhibitors and PROTAC degraders. *Eur J Med Chem* 2020;**204**:112657.
123. Yuan X, Bu H, Zhou J, Yang CY, Zhang H. Recent advances of SHP2 inhibitors in cancer therapy: current development and clinical application. *J Med Chem* 2020;**63**:11368−96.
124. Bagdanoff JT, Chen Z, Acker M, Chen YN, Chan H, Dore M, et al. Optimization of fused bicyclic allosteric SHP2 inhibitors. *J Med Chem* 2019;**62**:1781−92.
125. Andrews KT, Haque A, Jones MK. HDAC inhibitors in parasitic diseases. *Immunol Cell Biol* 2012;**90**:66−77.
126. Chaal BK, Gupta AP, Wastuwidyaningtyas BD, Luah YH, Bozdech Z. Histone deacetylases play a major role in the transcriptional regulation of the *Plasmodium falciparum* life cycle. *PLoS Pathog* 2010;**6**:e1000737.
127. Huang Z, Li R, Tang T, Ling D, Wang M, Xu D, et al. A novel multistage antiplasmodial inhibitor targeting *Plasmodium falciparum* histone deacetylase 1. *Cell Discov* 2020;**6**:93.
128. Li R, Ling D, Tang T, Huang Z, Wang M, Ding Y, et al. Discovery of novel *Plasmodium falciparum* HDAC1 inhibitors with dual-stage antimalarial potency and improved safety based on the clinical anticancer drug candidate quisinostat. *J Med Chem* 2021;**64**:2254−71.
129. Wang M, Tang T, Li R, Huang Z, Ling D, Zheng L, et al. Drug repurposing of quisinostat to discover novel plasmodium falciparum HDAC1 inhibitors with enhanced triple-stage antimalarial activity and improved safety. *J Med Chem* 2022;**65**:4156−81.
130. Escobar AS, Gardner JA, Sheth AG, Manfredi GG, Yang GO, Ouerfelli OML, et al. Inhibition of human peptide deformylase disrupts mitochondrial function. *Mol Cell Biol* 2010;**30**:5099−109.
131. Lee MD, Antczak CY, Li FM, Sirotnak WG, Bornmann DA, Scheinberg DA. A new human peptide deformylase inhibitable by actinonin. *Biochem Biophys Res Commun* 2003;**312**:309−15.
132. Lee MD, She MJ, Soskis CP, Borella JR, Gardner PA, Hayes BM, et al. Human mitochondrial peptide deformylase, a new anticancer target of actinonin-based antibiotics. *J Clin Invest* 2004;**114**:1107−16.

133. Chen DZ, Patel CJ, Hackbarth W, Wang G, Dreyer DC, Young PS, et al. Actinonin, a naturally occurring antibacterial agent, is a potent deformylase inhibitor. *Biochemistry* 2000;**39**:1256−62.
134. Hu L, Cai X, Dong S, Zhen Y, Hu J, Wang S, et al. Synthesis and anticancer activity of novel actinonin derivatives as HsPDF inhibitors. *J Med Chem* 2020;**63**:6959−78.
135. Mallinson J, Collins I. Macrocycles in new drug discovery. *Future Med Chem* 2012;**4**:1409−38.
136. Vendeville S, Cummings MD. Synthetic macrocycles in small molecule drug discovery. *Annu Rep Med Chem* 2013;**48**:371−86.
137. Cui JJ, Tran-Dubé M, Shen H, Nambu M, Kung PP, Pairish M, et al. Structure based drug design of crizotinib (PF-02341066), a potent and selective dual inhibitor of mesenchymal−epithelial transition factor (c-MET) kinase and anaplastic lymphoma kinase (ALK). *J Med Chem* 2011;**54**:6342−63.
138. Johnson TW, Richardson PF, Bailey S, Brooun A, Burke BJ, Collins MR, et al. Discovery of (10*R*)-7-amino-12-fluoro-2,10,16-trimethyl-15-oxo-10,15,16,17-tetrahydro-2*H*-8,4-(metheno)pyrazolo[4,3-*h*][2,5,11]-benzoxadiazacyclotetradecine-3-carbonitrile (PF-06463922), a macrocyclic inhibitor of anaplastic lymphoma kinase (ALK) and c-ROS oncogene 1 (ROS1) with preclinical brain exposure and broad-spectrum potency against ALK-resistant mutations. *J Med Chem* 2014;**57**:4720−44.
139. Cardenas MG, Oswald E, Yu W, Xue F, MacKerell Jr AD, Melnick AM. The expanding role of the BCL6 oncoprotein as a cancer therapeutic target. *Clin Cancer Res* 2017;**23**:885−93.
140. McCoull W, Abrams RD, Anderson E, Blades K, Barton P, Box M, et al. Discovery of pyrazolo[1,5-*a*]pyrimidine B-cell lymphoma 6 (BCL6) binders and optimization to high affinity macrocyclic inhibitors. *J Med Chem* 2017;**60**:4386−402.
141. Midha A, Dearden S, McCormack R. EGFR mutation incidence in non-small-cell lung cancer of adenocarcinoma histology: a systematic review and global map by ethnicity (mutMapII). *Am J Cancer Res* 2015;**5**:2892−911.
142. Zhang H, Yang X, Song Y, Yu B. Combining EGFR inhibitors with SHP2 or LSD1 inhibitors to overcome multidrug resistance in cancer. *Future Med Chem* 2022;**14**:527−9.
143. Konduri K, Gallant JN, Chae YK, Giles FJ, Gitlitz BJ, Gowen K, et al. EGFR fusions as novel therapeutic targets in lung cancer. *Cancer Discov* 2016;**6**:601−11.
144. Engelhardt H, Bose D, Petronczki M, Scharn D, Bader G, Baum A, et al. Start selective and rigidify: the discovery path toward a next generation of EGFR tyrosine kinase inhibitors. *J Med Chem* 2019;**62**:10272−93.
145. Chen H, Lai M, Zhang T, Chen Y, Tong L, Zhu S, et al. Conformational constrained 4-(1-sulfonyl-3-indol)yl-2-phenylaminopyrimidine derivatives as new fourth-generation epidermal growth factor receptor inhibitors targeting T790M/C797S mutations. *J Med Chem* 2022;**65**:6840−58.
146. Emsley J, McEwan PA, Gailani D. Structure and function of factor XI. *Blood* 2010;**115**:2569−77.
147. Gailani D, Renné T. Intrinsic pathway of coagulation and arterial thrombosis. *Arterioscler Thromb Vasc Biol* 2007;**27**:2507−13.
148. Pinto DJ, Smallheer JM, Corte JR, Austin EJ, Wang C, Fang T, et al. Structure-based design of inhibitors of coagulation factor XIa with novel P1 moieties. *Bioorg Med Chem Lett* 2015;**25**:1635−42.
149. Corte JR, Fang T, Osuna H, Pinto DJ, Rossi KA, Myers Jr JE, et al. Structure-based design of macrocyclic factor XIa inhibitors: discovery of the macrocyclic amide linker. *J Med Chem* 2017;**60**:1060−75.
150. Xu X, Meng Y, Li L, Xu P, Wang J, Li Z, et al. Overview of the development of glutaminase inhibitors: achievements and future directions. *J Med Chem* 2019;**62**:1096−115.
151. Gross MI, Demo SD, Dennison JB, Chen L, Chernov-Rogan T, Goyal B, et al. Antitumor activity of the glutaminase inhibitor CB-839 in triple-negative breast cancer. *Mol Cancer Ther* 2014;**13**:890−901.
152. Thangavelu K, Pan CQ, Karlberg T, Balaji G, Uttamchandani M, Suresh V, et al. Structural basis for the allosteric inhibitory mechanism of human kidney-type glutaminase (KGA) and its regulation by Raf-Mek-Erk signaling in cancer cell metabolism. *Proc Natl Acad Sci U S A* 2012;**109**:7705−10.
153. Xu X, Wang J, Wang M, Yuan X, Li L, Zhang C, et al. Structure-enabled discovery of novel macrocyclic inhibitors targeting glutaminase 1 allosteric binding site. *J Med Chem* 2021;**64**:4588−611.
154. Zack TI, Schumacher SE, Carter SL, Cherniack AD, Saksena G, Tabak B, et al. Pan-cancer patterns of somatic copy number alteration. *Nat Genet* 2013;**45**:1134−40.
155. Soderquist R, Eastman A. BCL2 Inhibitors as anticancer drugs: a plethora of misleading BH3 mimetics. *Mol Cancer Ther* 2016;**15**:2011−7.
156. Tron AE, Belmonte MA, Adam A, Aquila BM, Boise LH, Chiarparin E, et al. Discovery of Mcl-1-specific inhibitor AZD5991 and preclinical activity in multiple myeloma and acute myeloid leukemia. *Nat Commun* 2018;**9**:5341.
157. He M, Cao C, Ni Z, Liu Y, Song P, Hao S, et al. PROTACs: great opportunities for academia and industry (an update from 2020 to 2021). *Signal Transduct Target Ther* 2022;**7**:181.
158. Li X, Yao Y, Wu F, Song Y. A proteolysis-targeting chimera molecule selectively degrades ENL and inhibits malignant gene expression and tumor growth. *J Hematol Oncol* 2022;**15**:41.
159. McCoull W, Cheung T, Anderson E, Barton P, Burgess J, Byth K, et al. Development of a novel B-cell lymphoma 6 (BCL6) PROTAC to provide insight into small molecule targeting of BCL6. *ACS Chem Biol* 2018;**13**:3131−41.
160. Testa A, Hughes SJ, Lucas X, Wright JE, Ciulli A. Structure-based design of a macrocyclic PROTAC. *Angew Chem Int Ed* 2020;**59**:1727−34.
161. Gadd MS, Testa A, Lucas X, Chan KH, Chen W, Lamont DJ, et al. Structural basis of PROTAC cooperative recognition for selective protein degradation. *Nat Chem Biol* 2017;**13**:514−21.
162. Zengerle M, Chan KH, Ciulli A. Selective small molecule induced degradation of the BET bromodomain protein BRD4. *ACS Chem Biol* 2015;**10**:1770−7.